INTERNATIONAL JOURNAL FOR NUMERICAL METHODS IN FLUIDS
Int. J. Numer. Meth. Fluids 2008; **56**:1731–1764
Published online 29 August 2007 in Wiley InterScience (www.interscience.wiley.com). DOI: 10.1002/fld.1576

Preserving bounded and conservative solutions of transport in one-dimensional shallow-water flow with upwind numerical schemes: Application to fertigation and solute transport in rivers

J. Burguete[1,*,†], P. García-Navarro[2] and J. Murillo[2]

[1]*Suelo y Agua, Estación Experimental Aula Dei, CSIC, Zaragoza, Spain*
[2]*Fluid Mechanics, CPS, University of Zaragoza, Zaragoza, Spain*

SUMMARY

This work intends to show that conservative upwind schemes based on a separate discretization of the scalar solute transport from the shallow-water equations are unable to preserve uniform solute profiles in situations of one-dimensional unsteady subcritical flow. However, the coupled discretization of the system is proved to lead to the correct solution in first-order approximations. This work is also devoted to show that, when using a coupled discretization, a careful definition of the flux limiter function in second-order TVD schemes is required in order to preserve uniform solute profiles. The work shows that, in cases of subcritical irregular flow, the coupled discretization is necessary but nevertheless not sufficient to ensure concentration distributions free from oscillations and a method to avoid these oscillations is proposed. Examples of steady and unsteady flows in test cases, river and irrigation are presented. Copyright © 2007 John Wiley & Sons, Ltd.

Received 15 March 2007; Revised 18 June 2007; Accepted 19 June 2007

KEY WORDS: one-dimensional flow; advection–diffusion; conservation; numerical models; river flow; surface irrigation; upwind scheme

1. INTRODUCTION

The prediction of solute mixing occurring along a stream of water is important in many applications such as environmental or fertigation studies. The diffuse or the point release of a substance in water is transported along the flow leading to a solute concentration distribution that affects in different forms at different distances downstream from the input. The mechanics of mixing is complex and, consequently, practical problems are tackled using a number of assumptions and simplifications. In the most general problem, advection and turbulent diffusion occur in each of the

*Correspondence to: J. Burguete, Suelo y Agua, Estación Experimental Aula Dei, CSIC, Zaragoza, Spain.
†E-mail: jburguete@eead.csic.es

three coordinate directions. However, in the cases where a one-dimensional flow model is justified, such as river or channel flow, a tracer originating from a non-steady point source eventually mixes across the channel due to velocity gradients and turbulence and in the far field, a cross-sectional averaged concentration can be defined which is not subject to vertical and transverse concentration gradients. The fate of this cross-sectional averaged tracer concentration is then governed by a one-dimensional advection–dispersion equation [1, 2].

The dynamics of the one-dimensional flow and solute concentration can be studied using a system of conservation laws that requires appropriate numerical methods. In the last decades, shock-capturing finite volume schemes of different orders of accuracy for shallow-water equations based on approximate Riemann solvers and well balanced to properly incorporate the influence of bed variations and friction terms have been successfully reported [3–6]. The correct extension of these techniques to include the advection–dispersion equation is also one of the main goals of this work.

To obtain an accurate solution of the advective part of the transport process, a non-diffusive numerical scheme is required. To satisfy this requirement, some authors have used semi-Lagrangian schemes [7–9]. This option is linked to a decoupled discretization, in which the flow is solved using a different technique. An alternative is to use Eulerian schemes of the appropriate order for the separate system of equations [10–12]. Furthermore, Eulerian schemes can also be applied to the coupled set of equations [13]. The two last options are analysed in this work.

A one-dimensional shallow-water model including solute transport is formulated both forming a coupled and a decoupled system of equations. It is necessary as a first requirement to evaluate to what extent numerical schemes are able to preserve uniform initial solute profiles in irregular geometries or unsteady flow conditions. As a second goal, a suitable conservative scheme must be able to ensure bounded concentration values. It is not a trivial task since the solute concentration is not one of the conserved variables in our equation system. Several upwind finite volume techniques are presented and a few options considered for their numerical resolution.

The advection–diffusion of a gaussian profile with analytical solution is used as a test case to evaluate the performance of all the schemes discussed. Next the ideal dambreak unsteady flow with uniform solute concentration and solute discontinuity is used to evaluate the ability of the methods to preserve good properties in the solute distributions. Furthermore, a dambreak flow over sloping and rough bed is used for evaluating the ability of the numerical schemes and approximations to advect an initial square pulse of concentration. Two practical applications of solute transport, unsteady flow and solute transport on an impervious irrigation border and pollutant spill in a river, are finally presented.

2. FLOW AND TRANSPORT EQUATIONS

The one-dimensional system formed by the cross-sectional averaged liquid mass conservation, momentum balance in the mainstream direction and solute transport can be expressed in conservation form as

$$\frac{\partial \mathbf{U}}{\partial t} + \frac{\partial \mathbf{F}^{\mathrm{c}}}{\partial x} + \frac{\partial \mathbf{D}}{\partial x} = \mathbf{S}^{\mathrm{c}} \tag{1}$$

DOI: 10.1002/fld

where $\mathbf{U}$ is the vector of conserved variables, $\mathbf{F}^{\mathrm{c}}$ the flux vector, $\mathbf{S}^{\mathrm{c}}$ the source term vector, and $\mathbf{D}$ the diffusion:

$$\mathbf{U}=\begin{pmatrix} A \\ Q \\ As \end{pmatrix}, \quad \mathbf{F}^{\mathrm{c}}=\begin{pmatrix} Q \\ gI_1+\dfrac{\beta Q^2}{A} \\ Qs \end{pmatrix}, \quad \mathbf{S}^{\mathrm{c}}=\begin{pmatrix} 0 \\ g[I_2+A(S_0-S_{\mathrm{f}})] \\ 0 \end{pmatrix}$$
$$\mathbf{D}=\begin{pmatrix} 0 \\ 0 \\ -KA\dfrac{\partial s}{\partial x} \end{pmatrix} \tag{2}$$

with A being the wetted cross-section, Q the discharge, s the cross-sectional average solute concentration, g the gravity constant, S_0 the longitudinal bottom slope, S_{f} the longitudinal friction slope, K the diffusion coefficient, and I_1 and I_2 the pressure forces

$$I_1=\int_0^h (h-z)b\,\mathrm{d}z, \quad I_2=\int_0^h (h-z)\frac{\partial b}{\partial x}\,\mathrm{d}z \tag{3}$$

with h being the water depth, b the cross-sectional width, and β a coefficient resulting from the cross-sectional averaging of the velocity

$$\beta=\frac{A}{Q^2}\int_A v_x^2\,\mathrm{d}A \tag{4}$$

where v_x is the longitudinal component of the velocity at any point of the cross-section. From the average definition, $\beta \geqslant 1$. When the flow velocity can be considered uniform in the cross-section, as in all the examples presented in this work, $\beta \approx 1$. However, in cases of irregular or compound cross-sections, it is known that β can reach to values considerably larger so that a model for the velocity distribution in the cross-section must be used as in [14, 15].

The friction slope is widely modelled using of the Gauckler–Manning law [16, 17]:

$$S_{\mathrm{f}}=\frac{n^2 Q|Q|P^{4/3}}{A^{10/3}} \tag{5}$$

where P is the cross-sectional wetted perimeter and n the Gauckler–Manning roughness coefficient. The diffusion coefficient contains all the information related to molecular or viscous diffusion, turbulent diffusion and dispersion derived from the cross-sectional and turbulent averaging process. The model proposed by Rutherford [2] will be used

$$K=10\sqrt{gPA|S_{\mathrm{f}}|} \tag{6}$$

The system of equations can be expressed in a non-conservative form by taking into account

$$\frac{\mathrm{d}\mathbf{F}^{\mathrm{c}}(x,\mathbf{U})}{\mathrm{d}x}=\frac{\partial \mathbf{F}^{\mathrm{c}}}{\partial x}+\mathbf{J}\frac{\partial \mathbf{U}}{\partial x} \tag{7}$$

DOI: 10.1002/fld

with **J** being the flux Jacobian

$$\mathbf{J}=\frac{\partial \mathbf{F}^{\mathrm{c}}}{\partial \mathbf{U}}=\begin{pmatrix} 0 & 1 & 0 \\ c^2-\beta u^2 & 2\beta u & 0 \\ -us & s & u \end{pmatrix} \tag{8}$$

where $u=Q/A$ is the cross-sectional average velocity, $c=\sqrt{gA/B}$ the velocity of the infinitesimal waves and B the cross-sectional top width. Inserting in (1)

$$\frac{\partial \mathbf{U}}{\partial t}+\mathbf{J}\frac{\partial \mathbf{U}}{\partial x}+\frac{\partial \mathbf{D}}{\partial x}=\mathbf{S}^{\mathrm{nc}} \tag{9}$$

with $\mathbf{S}^{\mathrm{nc}}$ being the non-conservative source term

$$\mathbf{S}^{\mathrm{nc}}=\mathbf{S}^{\mathrm{c}}-\frac{\partial \mathbf{F}^{\mathrm{c}}}{\partial x}=\begin{pmatrix} 0 \\ c^2\dfrac{\partial A}{\partial x}-Au^2\dfrac{\partial \beta}{\partial x}-gA\left(\dfrac{\partial z_{\mathrm{s}}}{\partial x}+S_{\mathrm{f}}\right) \\ 0 \end{pmatrix} \tag{10}$$

where z_{s} is the water surface level.

The Jacobian matrix can be made diagonal

$$\mathbf{J}=\mathbf{P}\mathbf{\Lambda}\mathbf{P}^{-1},\quad \mathbf{P}=\begin{pmatrix} 1 & 1 & 0 \\ \lambda_1 & \lambda_2 & 0 \\ s & s & 1 \end{pmatrix},\quad \mathbf{\Lambda}=\begin{pmatrix} \lambda_1 & 0 & 0 \\ 0 & \lambda_2 & 0 \\ 0 & 0 & \lambda_3 \end{pmatrix} \tag{11}$$

with $\mathbf{\Lambda}$ being the eigenvalues diagonal matrix, **P** the diagonalizer matrix and λ_i the Jacobian eigenvalues corresponding to the characteristic propagation celerities

$$\lambda_1=\beta u+\sqrt{c^2+(\beta^2-\beta)u^2},\quad \lambda_2=\beta u-\sqrt{c^2+(\beta^2-\beta)u^2},\quad \lambda_3=u \tag{12}$$

The eigenvalues are related to the flow regime:

- $\lambda_1\lambda_2>0 \Rightarrow \beta u^2>c^2 \Rightarrow$ supercritical flow.
- $\lambda_1\lambda_2<0 \Rightarrow \beta u^2<c^2 \Rightarrow$ subcritical flow.

By defining the differential characteristic variables d**W** as

$$\mathrm{d}\mathbf{W}=\mathbf{P}^{-1}\,\mathrm{d}\mathbf{U} \tag{13}$$

and left-multiplying the non-conservative equation (9) by $\mathbf{P}^{-1}$, the characteristic differential equations are obtained:

$$\frac{\partial \mathbf{W}}{\partial t}+\mathbf{\Lambda}\frac{\partial \mathbf{W}}{\partial x}+\mathbf{P}^{-1}\frac{\partial \mathbf{D}}{\partial x}=\mathbf{P}^{-1}\mathbf{S}^{\mathrm{nc}} \tag{14}$$

Lastly, a simple and very convenient form of the equations is the quasi-conservative form. Taking into account that

$$\frac{\mathrm{d}I_1}{\mathrm{d}x}=I_2+A\frac{\mathrm{d}z_{\mathrm{s}}}{\mathrm{d}x} \tag{15}$$

DOI: 10.1002/fld

and inserting in (1)

$$\frac{\partial \mathbf{U}}{\partial t} + \frac{\partial \mathbf{F}^{\mathrm{qc}}}{\partial x} + \frac{\partial \mathbf{D}}{\partial x} = \mathbf{S}^{\mathrm{qc}} \tag{16}$$

with $\mathbf{F}^{\mathrm{qc}}$ and $\mathbf{S}^{\mathrm{qc}}$ being the quasi-conservative flux and source terms

$$\mathbf{F}^{\mathrm{qc}} = \begin{pmatrix} Q \\ \dfrac{\beta Q^2}{A} \\ Qs \end{pmatrix}, \quad \mathbf{S}^{\mathrm{qc}} = \begin{pmatrix} 0 \\ -gA\left(\dfrac{\mathrm{d}z_{\mathrm{s}}}{\mathrm{d}x} + S_{\mathrm{f}}\right) \\ 0 \end{pmatrix} \tag{17}$$

It must be stressed that, under form (16), the equations do not furnish the correct propagation information. The Jacobian matrix of the quasi-conservative form is

$$\mathbf{J}^{\mathrm{qc}} = \frac{\partial \mathbf{F}^{\mathrm{qc}}}{\partial \mathbf{U}} = \begin{pmatrix} 0 & 1 & 0 \\ -\beta u^2 & 2\beta u & 0 \\ -us & s & u \end{pmatrix} \tag{18}$$

with the eigenvalues

$$\lambda_1 = (\beta + \sqrt{\beta^2 - \beta})u, \quad \lambda_2 = (\beta - \sqrt{\beta^2 - \beta})u, \quad \lambda_3 = u \tag{19}$$

that do not correspond to the characteristic celerities of propagation of the information in this medium as in (12).

3. SEPARATE DISCRETIZATION OF THE SOLUTE TRANSPORT EQUATION

The simplest and most common method to solve the system of equations (2) is to discretize the mass and momentum flow equations separately, in each time step, from the solute transport equation. Keeping aside the method applied to the flow equations, let us consider the conservative form of the transport equation

$$\frac{\partial U}{\partial t} + \frac{\partial F}{\partial x} = 0 \tag{20}$$

$U = As$ being the conserved variable and $F = uAs - KA(\partial s/\partial x)$ the flux. This flux can be decomposed into a flux T due to advection and another flux D due to diffusion. In this case,

$$F = T + D, \quad T = uAs, \quad D = -KA\frac{\partial s}{\partial x} \tag{21}$$

we shall next concentrate on the description and discussion of different numerical methods suitable for the discretization of this equation alone.

DOI: 10.1002/fld

3.1. First-order upwind scheme with implicit diffusion

Upwind schemes are based on a spatial discretization according to the sign of the characteristic celerities of propagation in the system. Hence, spatial derivatives are evaluated at every point using a computational cell larger than the correct region of influence of that point. Combining the first-order explicit upwind scheme applied with the advection and the centred implicit scheme to solve the diffusion, both in the conservative forms, the following scheme is obtained:

$$\Delta U_i^n = -\frac{\Delta t}{\delta x}[(\delta T^+)_{i-(1/2)}^n + (\delta T^-)_{i+(1/2)}^n + D_{i+(1/2)}^{n+\theta} - D_{i-(1/2)}^{n+\theta}] \tag{22}$$

with δT^+ and δT^- associated with propagation velocities positive and negative, respectively,

$$u^\pm = \tfrac{1}{2}(u \pm |u|), \quad \delta T^\pm = \frac{u^\pm}{u}\delta T \tag{23}$$

where the notation $f^{n+\theta} = \theta f^{n+1} + (1-\theta) f^n$ has been used.

3.2. Second order in space TVD scheme with implicit diffusion

Combining the second order in space TVD explicit scheme applied to the advection and the centred implicit scheme to solve the diffusion, both in the conservative form, the following second order in space TVD semi-implicit scheme is obtained:

$$\Delta U_i^n = -\frac{\Delta t}{\delta x}\left\{(\delta T^+)_{i-(1/2)}^n + (\delta T^-)_{i+(1/2)}^n + D_{i+(1/2)}^{n+\theta} - D_{i-(1/2)}^{n+\theta} + \frac{1}{2}[(\Psi^+ \delta T^+)_{i-(1/2)}^n - (\Psi^+ \delta T^+)_{i-(3/2)}^n + (\Psi^- \delta T^-)_{i+(1/2)}^n - (\Psi^- \delta T^-)_{i+(3/2)}^n]\right\} \tag{24}$$

where Ψ^+ and Ψ^- are the flux limiter functions that are defined to combine the second-order spatial-centred and upwind schemes, to preserve the second order and, according to properties (A21), to avoid the numerical oscillations. In order to produce a second-order scheme, the dependence of flux limiter functions is defined as follows [18]:

$$\Psi_{i+(1/2)}^+ = \Psi\left(\frac{\delta T_{i+(3/2)}^+}{\delta T_{i+(1/2)}^+}\right), \quad \Psi_{i+(1/2)}^- = \Psi\left(\frac{\delta T_{i-(1/2)}^-}{\delta T_{i+(1/2)}^-}\right) \tag{25}$$

3.3. Second order in space and time TVD scheme with implicit diffusion

By combining the Sweby second order in space and time TVD explicit scheme [19] applied to the advection and the centred implicit scheme to solve the diffusion, both in conservative form, the following scheme is obtained:

$$\Delta U_i^n = -\frac{\Delta t}{\delta x}\left\{(\delta T^+)_{i-(1/2)}^n + (\delta T^-)_{i+(1/2)}^n + D_{i+(1/2)}^{n+\theta} - D_{i-(1/2)}^{n+\theta} + \frac{1}{2}[(\Psi^+ \delta E^+)_{i-(1/2)}^n - (\Psi^+ \delta E^+)_{i-(3/2)}^n + (\Psi^- \delta E^-)_{i+(1/2)}^n - (\Psi^- \delta E^-)_{i+(3/2)}^n]\right\} \tag{26}$$

DOI: 10.1002/fld

with

$$\delta E^{\pm} = (1 \mp \sigma)\delta T^{\pm}, \quad \sigma = u\frac{\Delta t}{\delta x}, \quad \sigma^{\pm} = \tfrac{1}{2}(\sigma \pm |\sigma|) \tag{27}$$

It is worth signalling that, although this scheme is named second order in space and time, this is not strictly true since it is not second order in time for the diffusion term. The dependence of the flux limiter functions is defined as [18]

$$\Psi^{+}_{i+(1/2)} = \Psi\left(\frac{(\delta E^{+})^{n}_{i+(3/2)}}{(\delta E^{+})^{n}_{i+(1/2)}}\right), \quad \Psi^{-}_{i+(1/2)} = \Psi\left(\frac{(\delta E^{-})^{n}_{i-(1/2)}}{(\delta E^{-})^{n}_{i+(1/2)}}\right) \tag{28}$$

4. COUPLED DISCRETIZATION OF THE SYSTEM

In what follows, our interest will be focused on the analysis of the discretization of the coupled system of equations using the most efficient techniques from Section 3: the first-order upwind and the second order in space and time TVD. Despite the apparently unnecessary extra complexity of this approach, it will prove to be the only method for improving the accuracy of the numerical solution in many cases, as previously reported [13].

4.1. First-order upwind scheme with implicit diffusion

According to the form of the scheme based on the characteristic form (A8), the following decomposition matrices are defined:

$$\mathbf{\Phi}^{\pm} = \begin{pmatrix} \phi_1^{\pm} & 0 & 0 \\ 0 & \phi_2^{\pm} & 0 \\ 0 & 0 & \phi_3^{\pm} \end{pmatrix} \tag{29}$$

and, at the same time, the upwind matrices associated with the propagation directions:

$$\phi_i^{\pm} = \tfrac{1}{2}[1 \pm \mathrm{sign}(\lambda_i)], \quad \mathbf{\Omega}^{\pm} = \mathbf{P}\mathbf{\Phi}^{\pm}\mathbf{P}^{-1}, \quad \mathbf{G}^{\pm} = \mathbf{\Omega}^{\pm}\mathbf{G} \tag{30}$$

In order to deal with transcritical problems in which the flow passes from subcritical to supercritical, the introduction of an artificial viscosity similar to the one proposed by Harten and Hyman [20] is necessary. This scheme becomes

$$\Delta\mathbf{U}_i^n = \Delta t\left[\left(\mathbf{G}^{+} - \nu\frac{\delta\mathbf{U}}{\delta x}\right)^{n}_{i-(1/2)} + \left(\mathbf{G}^{-} + \nu\frac{\delta\mathbf{U}}{\delta x}\right)^{n}_{i+(1/2)} - \frac{1}{\delta x}(\mathbf{D}^{n+\theta}_{i+(1/2)} - \mathbf{D}^{n+\theta}_{i-(1/2)})\right] \tag{31}$$

with ν an artificial viscosity coefficient defined as in [21]

$$\nu^{n}_{i+(1/2)} = \max_k \begin{cases} \tfrac{1}{4}[\delta(\lambda_k) - 2|\lambda_k|]^{n}_{i+(1/2)} & \text{if}(\lambda_k)^{n}_{i} < 0 \text{ and } (\lambda_k)^{n}_{i+1} > 0 \\ 0 & \text{otherwise} \end{cases} \tag{32}$$

Note that, for supercritical flow, $\mathbf{\Omega}^{+} = \mathbf{1}$, $\mathbf{\Omega}^{-} = \mathbf{0}$ and this discretization is identical to (22). The same is not true for subcritical flow.

DOI: 10.1002/fld

We shall postulate that the TVD condition for this combined scheme is governed by the most restrictive among the different eigenvalues, that is,

$$0\leqslant\theta\leqslant 1, \quad \Delta t\leqslant \min\left[\frac{\delta x}{\beta|u|+\sqrt{(\beta^2-\beta)u^2+c^2}}, \frac{\delta x^2}{|u|\delta x+(1-\theta)2K}\right] \tag{33}$$

4.2. Second order in space and time TVD scheme with implicit diffusion

The simplest form of extending the described scalar second order in space and time TVD scheme (26) to the coupled system of equations is

$$\Delta\mathbf{U}_i^n = \Delta t\left\{\left(\mathbf{G}^+ - \nu\frac{\delta\mathbf{U}}{\delta x}\right)^n_{i-(1/2)} + \left(\mathbf{G}^- + \nu\frac{\delta\mathbf{U}}{\delta x}\right)^n_{i+(1/2)} - \frac{1}{\delta x}(\mathbf{D}^{n+\theta}_{i+(1/2)} - \mathbf{D}^{n+\theta}_{i-(1/2)}) + \frac{1}{2}[(\boldsymbol{\Psi}^+\mathbf{E}^+)^n_{i-(1/2)} - (\boldsymbol{\Psi}^+\mathbf{E}^+)^n_{i-(3/2)} + (\boldsymbol{\Psi}^-\mathbf{E}^-)^n_{i+(1/2)} - (\boldsymbol{\Psi}^-\mathbf{E}^-)^n_{i+(3/2)}]\right\} \tag{34}$$

with the second-order vectors being

$$\mathbf{E}^\pm = \left(\mathbf{1}\mp\mathbf{J}\frac{\Delta t}{\delta x}\right)\mathbf{G}^\pm \tag{35}$$

The flux limiting matrices are defined as

$$\boldsymbol{\Psi}^\pm_{i+(1/2)} = \begin{pmatrix} \Psi\left(\dfrac{(\mathbf{E}^\pm)^1_{i+(1/2)\pm1}}{(\mathbf{E}^\pm)^1_{i+(1/2)}}\right) & 0 & 0 \\ 0 & \Psi\left(\dfrac{(\mathbf{E}^\pm)^2_{i+(1/2)\pm1}}{(\mathbf{E}^\pm)^2_{i+(1/2)}}\right) & 0 \\ 0 & 0 & \Psi\left(\dfrac{(\mathbf{E}^\pm)^3_{i+(1/2)\pm1}}{(\mathbf{E}^\pm)^3_{i+(1/2)}}\right) \end{pmatrix} \tag{36}$$

with $(\mathbf{E}^\pm)^i$ being the i component of vector $\mathbf{E}^\pm$. This new form of defining the flux limiting matrices, based on the components of the second-order vector, will be called vectorial limiting discretization.

Another alternative is to define the second-order vectors as

$$\mathbf{L}^\pm = \left(\mathbf{1}\mp\boldsymbol{\Lambda}^\pm\frac{\Delta t}{\delta x}\right)\mathbf{P}^{-1}\mathbf{G}^\pm \tag{37}$$

DOI: 10.1002/fld

Then, the second order in space and time TVD scheme is written as

$$\Delta \mathbf{U}_i^n = \Delta t \left\{ \left(\mathbf{G}^+ - v\frac{\delta \mathbf{U}}{\delta x} \right)_{i-(1/2)}^n + \left(\mathbf{G}^- + v\frac{\delta \mathbf{U}}{\delta x} \right)_{i+(1/2)}^n - \frac{1}{\delta x}(\mathbf{D}_{i+(1/2)}^{n+\theta} - \mathbf{D}_{i-(1/2)}^{n+\theta}) \right.$$
$$\left. + \frac{1}{2}[(\mathbf{P}\boldsymbol{\Psi}^+\mathbf{L}^+)_{i-(1/2)}^n - (\mathbf{P}\boldsymbol{\Psi}^+\mathbf{L}^+)_{i-(3/2)}^n + (\mathbf{P}\boldsymbol{\Psi}^-\mathbf{L}^-)_{i+(1/2)}^n - (\mathbf{P}\boldsymbol{\Psi}^-\mathbf{L}^-)_{i+(3/2)}^n] \right\} \tag{38}$$

and the flux limiting matrices are

$$\boldsymbol{\Psi}_{i+(1/2)}^{\pm} = \begin{pmatrix} \Psi\left(\dfrac{(\mathbf{L}^{\pm})_{i+(1/2)\pm 1}^1}{(\mathbf{L}^{\pm})_{i+(1/2)}^1} \right) & 0 & 0 \\ 0 & \Psi\left(\dfrac{(\mathbf{L}^{\pm})_{i+(1/2)\pm 1}^2}{(\mathbf{L}^{\pm})_{i+(1/2)}^2} \right) & 0 \\ 0 & 0 & \Psi\left(\dfrac{(\mathbf{L}^{\pm})_{i+(1/2)\pm 1}^3}{(\mathbf{L}^{\pm})_{i+(1/2)}^3} \right) \end{pmatrix} \tag{39}$$

This second form of defining the flux limiting matrices, more in the line of the characteristic form of scheme (A7), will be named characteristic limiting discretization.

Using that in the scalar case the TVD conditions for this scheme are identical to those for the first-order scheme, we shall postulate that this scheme is TVD whenever (33) holds.

5. PRESERVING BOUNDED SOLUTION SCHEMES

5.1. Preserving initial uniformity schemes

When the initial concentration as well as the boundary conditions are uniform, $(\partial s/\partial x = 0)$, the third of the conservation equations (1) becomes

$$\frac{\partial (As)}{\partial t} + \frac{\partial (Qs)}{\partial x} = \frac{\partial}{\partial x}\left(KA\frac{\partial s}{\partial x} \right) = 0 \tag{40}$$

By developing the derivatives and using the mass conservation equation

$$A\frac{\partial s}{\partial t} + s\left(\frac{\partial A}{\partial t} + \frac{\partial Q}{\partial x} \right) = 0 \;\Rightarrow\; \frac{\partial s}{\partial t} = 0 \tag{41}$$

indicating that, under these conditions, the concentration must stay constant in time whatever be the flow conditions. A numerical scheme unable to reproduce this important property will be unacceptable.

This case will be solved using the first-order upwind scheme with decoupled discretization, that is, solving in every time step first the system of mass and momentum flow equations (two

DOI: 10.1002/fld

first components of equation system (31)) and, separately, (22). With $\theta = 0$ and assuming positive discharges

$$\begin{aligned}\begin{pmatrix} A \\ Q \end{pmatrix}_i^{n+1} &= \begin{pmatrix} A \\ Q \end{pmatrix}_i^{n} - \Delta t \left\{ \left[\mathbf{\Omega}^- \frac{\delta}{\delta x} \begin{pmatrix} Q \\ H \end{pmatrix} \right]_{i+(1/2)}^{n} + \left[\mathbf{\Omega}^+ \frac{\delta}{\delta x} \begin{pmatrix} Q \\ H \end{pmatrix} \right]_{i-(1/2)}^{n} \right\} \\ (As)_i^{n+1} &= (As)_i^n - \frac{\Delta t}{\delta x}[(Qs)_i^n - (Qs)_{i-1}^n] + \frac{1}{\delta x}\left[\left(KA \frac{\delta s}{\delta x} \right)_{i+(1/2)}^{n} - \left(KA \frac{\delta s}{\delta x} \right)_{i-(1/2)}^{n} \right]\end{aligned} \tag{42}$$

where, in order to simplify the notation, the following has been defined:

$$\frac{\delta H}{\delta x} = gA\left(\frac{\delta z_s}{\delta x} + S_f \right) + \frac{\delta}{\delta x}\left(\frac{\beta Q^2}{A} \right) \tag{43}$$

With uniform concentration initial conditions $s_i^n = \text{const.} = s_0$

$$A_i^{n+1} s_i^{n+1} = A_i^n s_0 - s_0 \frac{\Delta t}{\delta x}(Q_i^n - Q_{i-1}^n) \tag{44}$$

In this case, the diagonalizer matrix is

$$\mathbf{P} = \begin{pmatrix} 1 & 1 \\ \lambda_1 & \lambda_2 \end{pmatrix} \tag{45}$$

For supercritical flow $\mathbf{\Omega}^+ = \mathbf{1}$, $\mathbf{\Omega}^- = \mathbf{0}$ so that

$$A_i^{n+1} = A_i^n - \frac{\Delta t}{\delta x}(Q_i^n - Q_{i-1}^n), \quad s_i^{n+1} = s_0 \tag{46}$$

therefore, the scheme is able to keep uniform the concentration for unsteady supercritical flows. However, in the case of subcritical flow

$$\begin{aligned}\mathbf{\Omega}^+ &= \mathbf{P}\begin{pmatrix} 1 & 0 \\ 0 & 0 \end{pmatrix}\mathbf{P}^{-1} = \frac{1}{\lambda_1 - \lambda_2}\begin{pmatrix} -\lambda_2 & 1 \\ -\lambda_1\lambda_2 & \lambda_1 \end{pmatrix} \\ \mathbf{\Omega}^- &= \mathbf{P}\begin{pmatrix} 0 & 0 \\ 0 & 1 \end{pmatrix}\mathbf{P}^{-1} = \frac{1}{\lambda_1 - \lambda_2}\begin{pmatrix} \lambda_1 & -1 \\ \lambda_2\lambda_1 & -\lambda_2 \end{pmatrix}\end{aligned} \tag{47}$$

so that

$$\begin{aligned}A_i^{n+1} &= A_i^n - \frac{\Delta t}{\delta x}\left[\left(\frac{-\lambda_2 \delta Q + \delta H}{\lambda_1 - \lambda_2} \right)_{i-(1/2)}^{n} + \left(\frac{\lambda_1 \delta Q - \delta H}{\lambda_1 - \lambda_2} \right)_{i+(1/2)}^{n} \right] \\ s_i^{n+1} &= \frac{A_i^n - \dfrac{\Delta t}{\delta x}(Q_i^n - Q_{i-1}^n)}{A_i^n - \dfrac{\Delta t}{\delta x}\left[\left(\dfrac{-\lambda_2 \delta Q + \delta H}{\lambda_1 - \lambda_2} \right)_{i-(1/2)}^{n} + \left(\dfrac{\lambda_1 \delta Q - \delta H}{\lambda_1 - \lambda_2} \right)_{i+(1/2)}^{n} \right]} s_0\end{aligned} \tag{48}$$

DOI: 10.1002/fld

Hence, for a general case, it cannot be assumed that $s_i^{n+1} = s_0$ and the scheme, although conservative and stable, produces a distortion in the uniform concentration distribution for unsteady subcritical flow. This is a non-trivial handicap for conservative schemes using decoupled discretization of the transport equation.

If the first-order upwind scheme is applied to the coupled system (31) with $\theta = 0$, assuming positive discharge and uniform concentration initial conditions

$$\begin{pmatrix} A \\ Q \\ As \end{pmatrix}_i^{n+1} = \begin{pmatrix} A \\ Q \\ As \end{pmatrix}_i^{n} - \Delta t \left\{ \left[\mathbf{\Omega}^- \frac{\delta}{\delta x} \begin{pmatrix} Q \\ H \\ T \end{pmatrix} \right]_{i+(1/2)}^{n} + \left[\mathbf{\Omega}^+ \frac{\delta}{\delta x} \begin{pmatrix} Q \\ H \\ T \end{pmatrix} \right]_{i-(1/2)}^{n} \right\} \tag{49}$$

In this case, $\mathbf{P}$ is defined as in (11). For supercritical flow $\mathbf{\Omega}^+ = \mathbf{1}$, $\mathbf{\Omega}^- = \mathbf{0}$ so that

$$A_i^{n+1} = A_i^n - \frac{\Delta t}{\delta x}(Q_i^n - Q_{i-1}^n), \quad s_i^{n+1} = s_0 \tag{50}$$

and the scheme reproduces the uniform concentration during the unsteady calculation. For subcritical flow

$$\begin{aligned} \mathbf{\Omega}^+ &= \mathbf{P} \begin{pmatrix} 1 & 0 & 0 \\ 0 & 0 & 0 \\ 0 & 0 & 1 \end{pmatrix} \mathbf{P}^{-1} = \frac{1}{\lambda_1 - \lambda_2} \begin{pmatrix} -\lambda_2 & 1 & 0 \\ -\lambda_1\lambda_2 & \lambda_1 & 0 \\ -\lambda_1 s & s & \lambda_1 - \lambda_2 \end{pmatrix} \\ \mathbf{\Omega}^- &= \mathbf{P} \begin{pmatrix} 0 & 0 & 0 \\ 0 & 1 & 0 \\ 0 & 0 & 0 \end{pmatrix} \mathbf{P}^{-1} = \frac{1}{\lambda_1 - \lambda_2} \begin{pmatrix} \lambda_1 & -1 & 0 \\ \lambda_1\lambda_2 & -\lambda_2 & 0 \\ \lambda_1 s & -s & 0 \end{pmatrix} \end{aligned} \tag{51}$$

so that

$$\begin{aligned} A_i^{n+1} &= A_i^n - \frac{\Delta t}{\delta x}\left[\left(\frac{-\lambda_2 \delta Q + \delta H}{\lambda_1 - \lambda_2} \right)_{i-(1/2)}^{n} + \left(\frac{\lambda_1 \delta Q - \delta H}{\lambda_1 - \lambda_2} \right)_{i+(1/2)}^{n} \right] \\ s_i^{n+1} &= \frac{A_i^n s_i^n - \dfrac{\Delta t}{\delta x}\left[\left(\dfrac{-\lambda_1 s \delta Q + s\delta H + (\lambda_1 - \lambda_2)\delta T}{\lambda_1 - \lambda_2} \right)_{i-(1/2)}^{n} + \left(\dfrac{\lambda_1 s \delta Q - s\delta H}{\lambda_1 - \lambda_2} \right)_{i+(1/2)}^{n} \right]}{A_i^n - \dfrac{\Delta t}{\delta x}\left[\left(\dfrac{-\lambda_2 \delta Q + \delta H}{\lambda_1 - \lambda_2} \right)_{i-(1/2)}^{n} + \left(\dfrac{\lambda_1 \delta Q - \delta H}{\lambda_1 - \lambda_2} \right)_{i+(1/2)}^{n} \right]} \\ &= \frac{A_i^n - \dfrac{\Delta t}{\delta x}\left[\left(\dfrac{-\lambda_2 \delta Q + \delta H}{\lambda_1 - \lambda_2} \right)_{i-(1/2)}^{n} + \left(\dfrac{\lambda_1 \delta Q - \delta H}{\lambda_1 - \lambda_2} \right)_{i+(1/2)}^{n} \right]}{A_i^n - \dfrac{\Delta t}{\delta x}\left[\left(\dfrac{-\lambda_2 \delta Q + \delta H}{\lambda_1 - \lambda_2} \right)_{i-(1/2)}^{n} + \left(\dfrac{\lambda_1 \delta Q - \delta H}{\lambda_1 - \lambda_2} \right)_{i+(1/2)}^{n} \right]} s_0 = s_0 \end{aligned} \tag{52}$$

and the scheme is also able to guarantee uniform concentration during the unsteady calculation.

It is easy to show that this also occurs while using the TVD schemes with characteristic limiting discretization (38). However, the vectorial limiting discretization (34) does not guarantee that

DOI: 10.1002/fld

the scheme preserves uniformity in the transported scalar distribution, see Figure 7. Hence, even though it might seem an unnecessary complication in the procedure, the coupled formulation of the system of equations and the characteristic limiting discretization are crucial to improve the quality of the solutions in unsteady solute transport problems.

5.2. Preserving bounded solution schemes

A little transformation in the conservative transport equation, that involves the use of the mass conservation equation, leads to the characteristic form of the transport equation:

$$\frac{\partial s}{\partial t} + u\frac{\partial s}{\partial x} = \frac{1}{A}\frac{\partial}{\partial x}\left(KA\frac{\partial s}{\partial x}\right) \tag{53}$$

In the absence of diffusion ($K = 0$), this is a scalar wave equation

$$\frac{\partial s}{\partial t} + u\frac{\partial s}{\partial x} = 0 \tag{54}$$

with exact solution given an initial solute distribution $s_0(x)$, representing the pure advection

$$s(x,t) = s_0\left(x - \int_0^t u(x',t')\,\mathrm{d}t'\right), \quad \frac{\mathrm{d}x'}{\mathrm{d}t'} = u(x',t') \tag{55}$$

Therefore, the solution of the equation contains the same extrema in concentration that are present in the initial conditions. The numerical schemes that have the property of being able to preserve this condition will be called 'preserving bounded solution' schemes. Obviously, the methods that do not preserve a uniform concentration are not able to meet these new property.

For instance, a discontinuous initial concentration distribution with uniform values at both sides of the discontinuity is represented in Figure 1. If a numerical scheme that preserves the bounded solution is sought, the following conditions must hold:

$$s_i^n \geqslant s_i^{n+1} \geqslant s_{i+1}^n, \quad s_i^n \geqslant s_i^{n+1} \geqslant s_{i+1}^{n+1} \tag{56}$$

We shall first consider the first-order upwind scheme with coupled discretization in order to study whether it meets (56). For supercritical flow ($\mathbf{G}^+ = \mathbf{G}$, $\mathbf{G}^- = \mathbf{0}$) in this case

$$\begin{aligned} A_i^{n+1} &= A_i^n - \frac{\Delta t}{\delta x}\delta Q_{i-(1/2)}^n, \quad (As)_i^{n+1} = (As)_i^n - \frac{\Delta t}{\delta x}\delta(Qs)_{i-(1/2)}^n \\ A_{i+1}^{n+1} &= A_{i+1}^n - \frac{\Delta t}{\delta x}\delta Q_{i+(1/2)}^n, \quad (As)_{i+1}^{n+1} = (As)_{i+1}^n - \frac{\Delta t}{\delta x}\delta(Qs)_{i+(1/2)}^n \end{aligned} \tag{57}$$

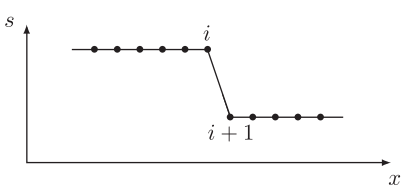

Figure 1. Discontinuous solute concentration distribution with a jump between nodes i and $i + 1$.

DOI: 10.1002/fld

Taking into account that

$$s_{i-1}^n = s_{i-(1/2)}^n = s_i^n \geqslant s_{i+1}^n = s_{i+(3/2)}^n = s_{i+2}^n \tag{58}$$

solving the solute concentrations in (57)

$$s_i^{n+1} = s_i^n, \quad s_{i+1}^{n+1} = \frac{(As)_{i+1}^n - \dfrac{\Delta t}{\delta x}[(Qs)_{i+1}^n - (Qs)_i^n]}{A_{i+1}^n - \dfrac{\Delta t}{\delta x}\delta Q_{i+(1/2)}^n} \tag{59}$$

This solution satisfies (56) since

$$\begin{aligned} s_{i+1}^{n+1} &= \frac{(As)_{i+1}^n - \dfrac{\Delta t}{\delta x}[(Qs)_{i+1}^n - (Qs)_i^n]}{A_{i+1}^n - \dfrac{\Delta t}{\delta x}\delta Q_{i+(1/2)}^n} \leqslant \frac{(As)_{i+1}^n - \dfrac{\Delta t}{\delta x}[(Qs)_{i+1}^n - Q_i^n s_{i+1}^n]}{A_{i+1}^n - \dfrac{\Delta t}{\delta x}\delta Q_{i+(1/2)}^n} = s_{i+1}^n \\ s_i^n \geqslant s_{i+1}^{n+1} &\Leftrightarrow s_i^n \left(A_{i+1}^n - \frac{\Delta t}{\delta x}\delta Q_{i+(1/2)}^n\right) \geqslant (As)_{i+1}^n - \frac{\Delta t}{\delta x}[(Qs)_{i+1}^n - (Qs)_i^n] \\ &\Leftrightarrow s_i^n \left(A - \frac{\Delta t}{\delta x}Q\right)_{i+1}^n \geqslant \left(A - \frac{\Delta t}{\delta x}Q\right)_{i+1}^n s_{i+1}^n \quad \Leftrightarrow \quad u_{i+1}^n \frac{\Delta t}{\delta x} \leqslant 1 \end{aligned} \tag{60}$$

and this holds whenever the scheme stability condition (33) holds.

In cases of subcritical flow, an artificial diffusion will be added to the first-order upwind scheme with coupled discretization so that even in the absence of physical diffusion, the following decomposition will be applied:

$$\mathbf{G}_{i+(1/2)}^{\mathrm{L}} = [\mathbf{G}^+ - \mathbf{V}]_{i+(1/2)}^n, \quad \mathbf{G}_{i+(1/2)}^{\mathrm{R}} = [\mathbf{G}^- + \mathbf{V}]_{i+(1/2)}^n, \quad \mathbf{V} = -\frac{1}{\delta x}\begin{pmatrix} 0 \\ 0 \\ \xi\delta s \end{pmatrix}_{i+(1/2)}^n \tag{61}$$

with ξ a strictly positive ($\xi \geqslant 0$) artificial diffusion coefficient. We shall next state the conditions over this parameter for the scheme to satisfy (56). Applying the scheme to our problem

$$\begin{aligned} A_i^{n+1} &= A_i^n - \frac{\Delta t}{\delta x}[(\delta Q^+)_{i-(1/2)}^n + (\delta Q^-)_{i+(1/2)}^n] \\ A_{i+1}^{n+1} &= A_{i+1}^n - \frac{\Delta t}{\delta x}[(\delta Q^+)_{i+(1/2)}^n + (\delta Q^-)_{i+(3/2)}^n] \\ (As)_i^{n+1} &= (As)_i^n - \frac{\Delta t}{\delta x}[\delta(Qs)_{i-(1/2)}^n - (s\delta Q^- - \xi\delta s)_{i-(1/2)}^n + (s\delta Q^- - \xi\delta s)_{i+(1/2)}^n] \\ (As)_{i+1}^{n+1} &= (As)_{i+1}^n - \frac{\Delta t}{\delta x}[\delta(Qs)_{i+(1/2)}^n - (s\delta Q^- - \xi\delta s)_{i+(1/2)}^n + (s\delta Q^- - \xi\delta s)_{i+(3/2)}^n] \end{aligned} \tag{62}$$

where, for the sake of simplicity in the notation, the following has been used:

$$\delta Q^+ = \frac{-\lambda_2\delta Q + \delta H}{\lambda_1 - \lambda_2}, \quad \delta Q^- = \frac{\lambda_1\delta Q - \delta H}{\lambda_1 - \lambda_2} \tag{63}$$

DOI: 10.1002/fld

Taking into account that

$$[\delta(Qs) - s\delta Q^-]^n_{i+(1/2)} = (Q\delta s + s\delta Q - s\delta Q^-)^n_{i+(1/2)} = (Q\delta s + s\delta Q^+)^n_{i+(1/2)} \tag{64}$$

using (58) and solving the concentrations:

$$\begin{aligned} s_i^{n+1} &= \frac{(As)_i^n - \dfrac{\Delta t}{\delta x}[s_i^n \delta(Q^+)^n_{i-(1/2)} + (s\delta Q^- - \xi\delta s)^n_{i+(1/2)}]}{A_i^n - \dfrac{\Delta t}{\delta x}[(\delta Q^+)^n_{i-(1/2)} + (\delta Q^-)^n_{i+(1/2)}]} \\ s_{i+1}^{n+1} &= \frac{(As)_{i+1}^n - \dfrac{\Delta t}{\delta x}[(Q\delta s)^n_{i+(1/2)} + (s\delta Q^+ + \xi\delta s)^n_{i+(1/2)} + s_{i+1}^n \delta(Q^-)^n_{i+(3/2)}]}{A_{i+1}^n - \dfrac{\Delta t}{\delta x}[(\delta Q^+)^n_{i+(1/2)} + (\delta Q^-)^n_{i+(3/2)}]} \end{aligned} \tag{65}$$

Substituting these expressions in conditions (56), the inequalities hold provided that

$$\begin{aligned} &\xi^n_{i+(1/2)} \geqslant (\delta Q^-)^n_{i+(1/2)} \frac{s^n_{i+(1/2)} - s^n_i}{s^n_{i+1} - s^n_i}, \quad \xi^n_{i+(1/2)} \geqslant -Q^n_{i+(1/2)} + (\delta Q^+)^n_{i+(1/2)} \frac{s^n_{i+1} - s^n_{i+(1/2)}}{s^n_{i+1} - s^n_i} \\ &\Delta t \leqslant \frac{A_i^{n+1}\delta x}{\xi^n_{i+(1/2)} - (\delta Q^-)^n_{i+(1/2)} \dfrac{s^n_{i+(1/2)} - s^n_i}{s^n_{i+1} - s^n_i}} \\ &\Delta t \leqslant \frac{A_{i+1}^{n+1}\delta x}{\xi^n_{i+(1/2)} + Q^n_{i+(1/2)} - (\delta Q^+)_{i+(1/2)} \dfrac{s^n_{i+1} - s^n_{i+(1/2)}}{s^n_{i+1} - s^n_i}} \end{aligned} \tag{66}$$

Hence, the artificial diffusion coefficient can be defined as

$$\xi^n_{i+(1/2)} = \begin{cases} \max\left[0, (\delta Q^-)^n_{i+(1/2)} \dfrac{s^n_{i+(1/2)} - s^n_i}{s^n_{i+1} - s^n_i}, \right. \\ \quad \left. -Q^n_{i+(1/2)} + (\delta Q^+)^n_{i+(1/2)} \dfrac{s^n_{i+1} - s^n_{i+(1/2)}}{s^n_{i+1} - s^n_i}\right] & \text{if } \beta u^2 < c^2 \\ 0 & \text{if } \beta u^2 \geqslant c^2 \end{cases} \tag{67}$$

Using this, the right-hand side quantities in the two last inequalities (66) are strictly positive, so that the scheme can meet all the necessary conditions to preserve the bounded solution by reducing the time step if necessary. It can also be proved that the same conditions also keep a solution bounded with the opposite sign in the discontinuity, that is,

$$s_i^n \leqslant s_i^{n+1} \leqslant s_{i+1}^n, \quad s_i^n \leqslant s_i^{n+1} \leqslant s_{i+1}^{n+1} \tag{68}$$

Since a series of discontinuities is a typical spatial approximation in a discretization, the above conditions can be considered sufficient for keeping bounded any initial distribution.

DOI: 10.1002/fld

Given that the second order in space and time TVD scheme reduces to the first-order upwind scheme in the vicinity of discontinuities, the same artificial diffusion coefficient will be applied. Then using, for instance, the characteristic limiting discretization of the flux limiter, the scheme with artificial diffusion is

$$\Delta \mathbf{U}_i^n = \Delta t \left\{ \left(\mathbf{G}^+ - \nu \frac{\delta \mathbf{U}}{\delta x} - \mathbf{V} \right)_{i-(1/2)}^n + \left(\mathbf{G}^- + \nu \frac{\delta \mathbf{U}}{\delta x} + \mathbf{V} \right)_{i+(1/2)}^n - \frac{1}{\delta x} (\mathbf{D}_{i+(1/2)}^{n+\theta} - \mathbf{D}_{i-(1/2)}^{n+\theta}) \right.$$
$$\left. + \frac{1}{2} [(\mathbf{P}\boldsymbol{\Psi}^+ \mathbf{L}^+)_{i-(1/2)}^n - (\mathbf{P}\boldsymbol{\Psi}^+ \mathbf{L}^+)_{i-(3/2)}^n + (\mathbf{P}\boldsymbol{\Psi}^- \mathbf{L}^-)_{i+(1/2)}^n - (\mathbf{P}\boldsymbol{\Psi}^- \mathbf{L}^-)_{i+(3/2)}^n] \right\} \tag{69}$$

6. BOUNDARY CONDITIONS

A correct numerical model for unsteady flow problems must be based not only on a conservative and accurate numerical scheme, but also on an adequate procedure to discretize the boundary conditions. The theory of characteristics provides clear indications about the number of necessary external boundary conditions to define a well-posed problem [18].

For the water flow, two external physical boundary conditions are required at the inlet and two numerical boundary conditions are required at the outlet in cases of supercritical flow; however, both a physical and a numerical boundary condition at the inlet and at the outlet are necessary in cases of subcritical flow. The most usual physical boundary conditions at the inlet are a discharge hydrograph $Q(t)$ or a water depth limnigraph $h(t)$ in the case of subcritical flow and both together $Q(t)$, $h(t)$ in the case of supercritical flow. At the outlet, the most common practices to use are a rating curve of the type $Q = Q(h)$ or a limnigraph $h(t)$. Critical outlet or closed outlet can be considered as particular cases. For the solute transport, a physical boundary condition at the inlet, the most usual being a concentration input $s(t)$, and a numerical boundary condition at the outlet are required.

The method of global mass conservation [22, 23] is based on enforcing the integral form of the mass conservation extended to all the computational domains in combination with a conservative scheme for the interior points to generate the numerical boundary condition. In a domain discretized using N cells, if a conservative scheme defined by a nodal flux $\mathbf{F}_i^{\mathrm{T}}$ is used all over the domain, the cross-sectional increments predicted in one time step are

$$\Delta A_i^n = -\frac{\Delta t}{\delta x} (\delta Q_{i+(1/2)}^{\mathrm{R}} + \delta Q_{i-(1/2)}^{\mathrm{L}}), \quad \Delta (As)_i^n = -\frac{\Delta t}{\delta x} (\delta T_{i+(1/2)}^{\mathrm{R}} + \delta T_{i-(1/2)}^{\mathrm{L}}) \tag{70}$$

Therefore, the total numerical water volume ΔV^n and solute mass ΔM^n variations produced by the scheme are, neglecting contributions from outside cells ($\delta \mathbf{F}_{1/2}^{\mathrm{L}} = \delta \mathbf{F}_{N+(1/2)}^{\mathrm{R}} = \mathbf{0}$),

$$\Delta V^n = \sum_{i=1}^{N} \Delta A_i^n \delta x = -\Delta t \sum_{i=1}^{N} (\delta Q_{i-(1/2)}^{\mathrm{L}} + \delta Q_{i+(1/2)}^{\mathrm{R}}) = \Delta t (Q_1^{\mathrm{T}} - Q_N^{\mathrm{T}})$$
$$\Delta M^n = \sum_{i=1}^{N} \Delta (As)_i^n \delta x = -\Delta t \sum_{i=1}^{N} (\delta T_{i-(1/2)}^{\mathrm{L}} + \delta T_{i+(1/2)}^{\mathrm{R}}) = \Delta t (T_1^{\mathrm{T}} - T_N^{\mathrm{T}}) \tag{71}$$

DOI: 10.1002/fld

Since the scheme used is conservative, the variations are only due to the boundaries and can be split into numerical contributions at the inlet and at the outlet in the following form:

$$\begin{aligned} \Delta V^n &= \Delta V^n_{\text{in}} + \Delta V^n_{\text{out}}, \quad \Delta V^n_{\text{in}} = \Delta t\, Q^{\text{T}}_1, \quad \Delta V^n_{\text{out}} = -\Delta t\, Q^{\text{T}}_N \\ \Delta M^n &= \Delta M^n_{\text{in}} + \Delta M^n_{\text{out}}, \quad \Delta M^n_{\text{in}} = \Delta t\, T^{\text{T}}_1, \quad \Delta M^n_{\text{out}} = -\Delta t\, T^{\text{T}}_N \end{aligned} \tag{72}$$

If the physical boundary condition are, for instance, a certain water volume ΔV^{phy} or solute mass ΔM^{phy} inputs at the inlet or at the outlet, in order to ensure the global mass conservation of the scheme, the numerical mass increments must be corrected. This is achieved by means of additional increments ΔA and $\Delta(As)$ at the inlet or at the outlet, that must be added to those previously obtained by the numerical scheme (70), so that

$$\begin{aligned} \Delta V^{\text{phy}}_{\text{in}} &= \Delta A^a_1 \delta x + \Delta t\, Q^{\text{T}}_1, \quad \Delta V^{\text{phy}}_{\text{out}} = \Delta A^a_N \delta x - \Delta t\, Q^{\text{T}}_N \\ \Delta M^{\text{phy}}_{\text{in}} &= \Delta (As)^a_1 \delta x + \Delta t\, T^{\text{T}}_1, \quad \Delta M^{\text{phy}}_{\text{out}} = \Delta (As)^a_N \delta x - \Delta t\, T^{\text{T}}_N \end{aligned} \tag{73}$$

Since all the schemes considered meet $\mathbf{F}^{\text{T}}_i = (\mathbf{F}^{\text{c}})^n_i$, the additional increments are

$$\begin{aligned} \Delta A^a_1 &= \frac{\Delta V^{\text{phy}}_{\text{in}} - \Delta t\, Q^n_1}{\delta x}, \quad \Delta A^a_N = \frac{\Delta V^{\text{phy}}_{\text{out}} + \Delta t\, Q^n_N}{\delta x} \\ \Delta (As)^a_1 &= \frac{\Delta M^{\text{phy}}_{\text{in}} - \Delta t\, (Qs)^n_1}{\delta x}, \quad \Delta (As)^a_N = \frac{\Delta M^{\text{phy}}_{\text{out}} + \Delta t\, (Qs)^n_N}{\delta x} \end{aligned} \tag{74}$$

More details on the use of these conditions in different particular cases can be found in [23].

7. ANALYTICAL SOLUTIONS TO THE ADVECTION–DIFFUSION EQUATION

7.1. Advection–diffusion of a gaussian profile

There are cases where the advection–diffusion equation can be solved analytically. These cases are very useful to validate the numerical solutions. Considering constant the cross-sectional area, the velocity and the diffusion coefficient as constants, the linearized equation is obtained:

$$\frac{\partial s}{\partial t} + u \frac{\partial s}{\partial x} = K \frac{\partial^2 s}{\partial x^2} \tag{75}$$

With an initial gaussian profile, analytical solutions to this equation can be obtained:

$$s(x, t) = s_0 + \frac{s_1}{\sqrt{1 + 4aKt}} \exp\left[-\frac{a(x - x_0 - ut)^2}{1 + 4aKt} \right] \tag{76}$$

We shall first consider a case of pure diffusion of a profile with $s_0 = 0.2\,\text{kg/m}^3$, $s_1 = 0.6\,\text{kg/m}^3$, $a = 0.04\,\text{m}^{-2}$, $u = 0\,\text{m/s}$, $K = 0.2\,\text{m}^2/\text{s}$ and $x_0 = 50\,\text{m}$ after 250 s, as represented in Figure 2(a), and the propagation of a profile with $s_0 = 0.1\,\text{kg/m}^3$, $s_1 = 0.8\,\text{kg/m}^3$, $a = 0.01\,\text{m}^{-2}$, $u = 1\,\text{m/s}$, $K = 0.2\,\text{m}^2/\text{s}$ and $x_0 = 20\,\text{m}$ after 60 s, as represented in Figure 2(b). To simulate the profiles,

DOI: 10.1002/fld

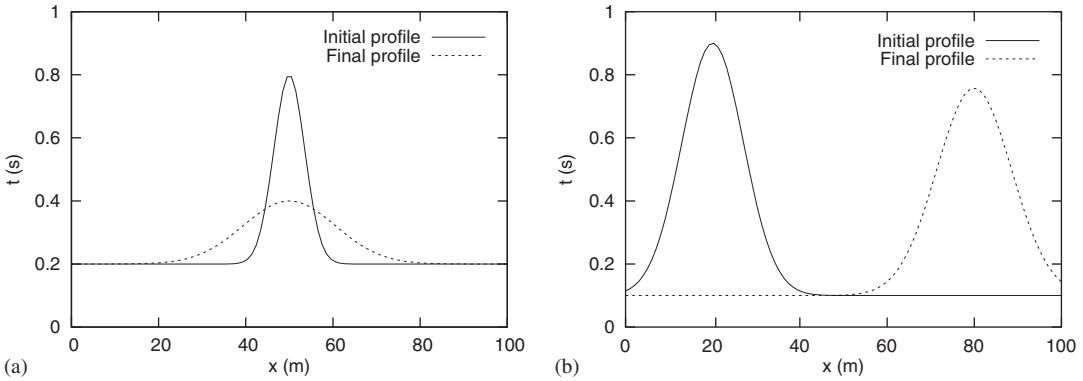

Figure 2. (a) Pure diffusion and (b) advection–diffusion of a gaussian profile.

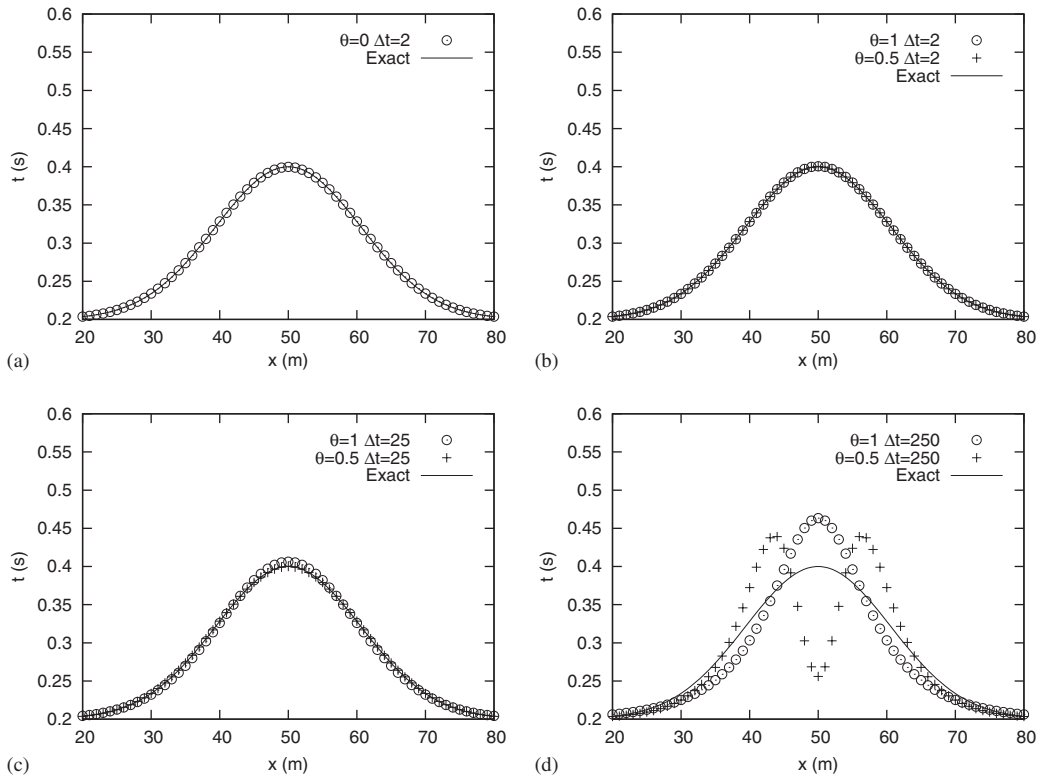

Figure 3. Pure diffusion of a gaussian profile with the implicit centred scheme for different values of θ and Δt.

a grid with $\delta x = 1$ m will be used. The numerical results for the pure diffusion case, shown in Figure 3, indicate that the explicit scheme is the most accurate for the diffusion. The implicit scheme with $\theta = 1$ presents a slight antidiffusive tendency that becomes more noticeable as the

DOI: 10.1002/fld

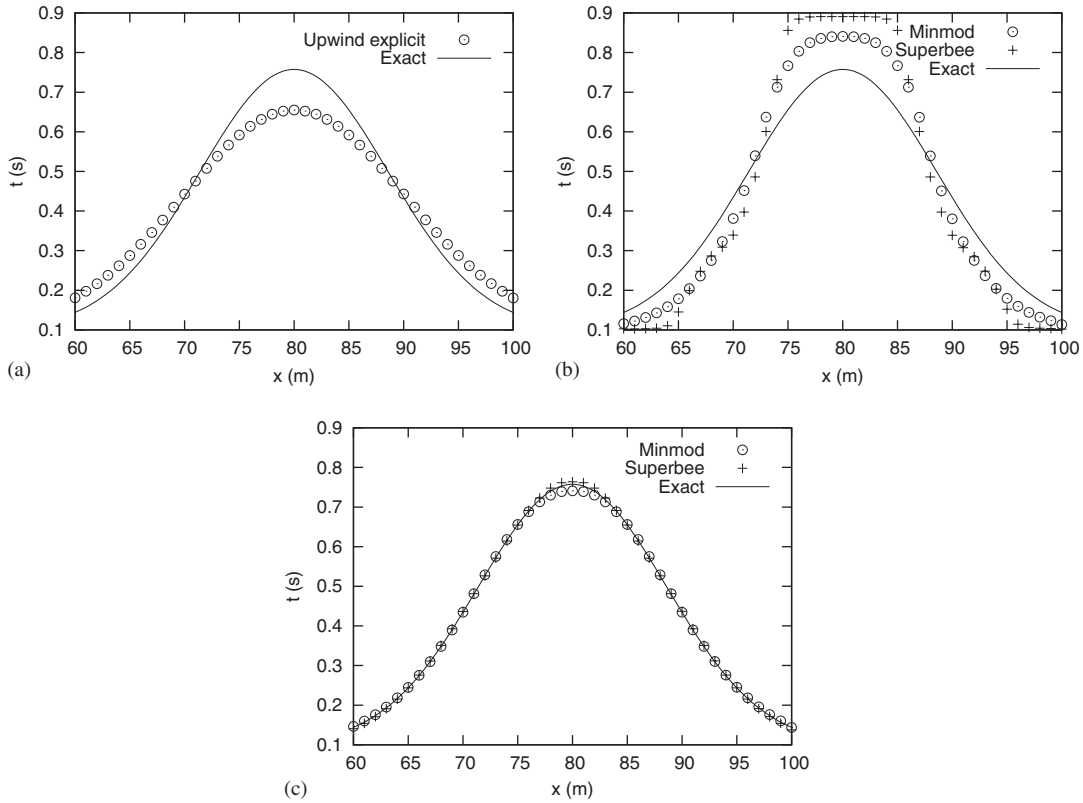

Figure 4. Advection–diffusion of a gaussian profile using the schemes: (a) first-order upwind explicit, (b) second-order in space TVD and (c) second order in space and time TVD with different time-step sizes. In (a)–(c) $\Delta t = 0.5$ s is used.

time-step size increases. The numerical antidiffusivity decreases with the parameter θ although, for large time steps, the TVD criterion can be violated in this case and numerical oscillations may appear (Figure 3(d)). In order to simultaneously avoid numerical oscillations and minimize the antidiffusivity, in what follows the smallest value of θ compatible with the TVD conditions (A26) and (A28) will be used:

- First order and second order in space and time TVD with implicit diffusion schemes

$$\theta = \max\left[0, 1 - \left(\frac{\delta x}{\Delta t} - |u|\right)\frac{\delta x}{2K}\right] \tag{77}$$

- Second order in space TVD with implicit diffusion scheme

$$\theta = \max\left\{0, 1 - \left[\frac{\delta x}{\Delta t} - |u|\left(1 + \frac{1}{2}\max(\Psi)\right)\right]\frac{\delta x}{2K}\right\} \tag{78}$$

DOI: 10.1002/fld

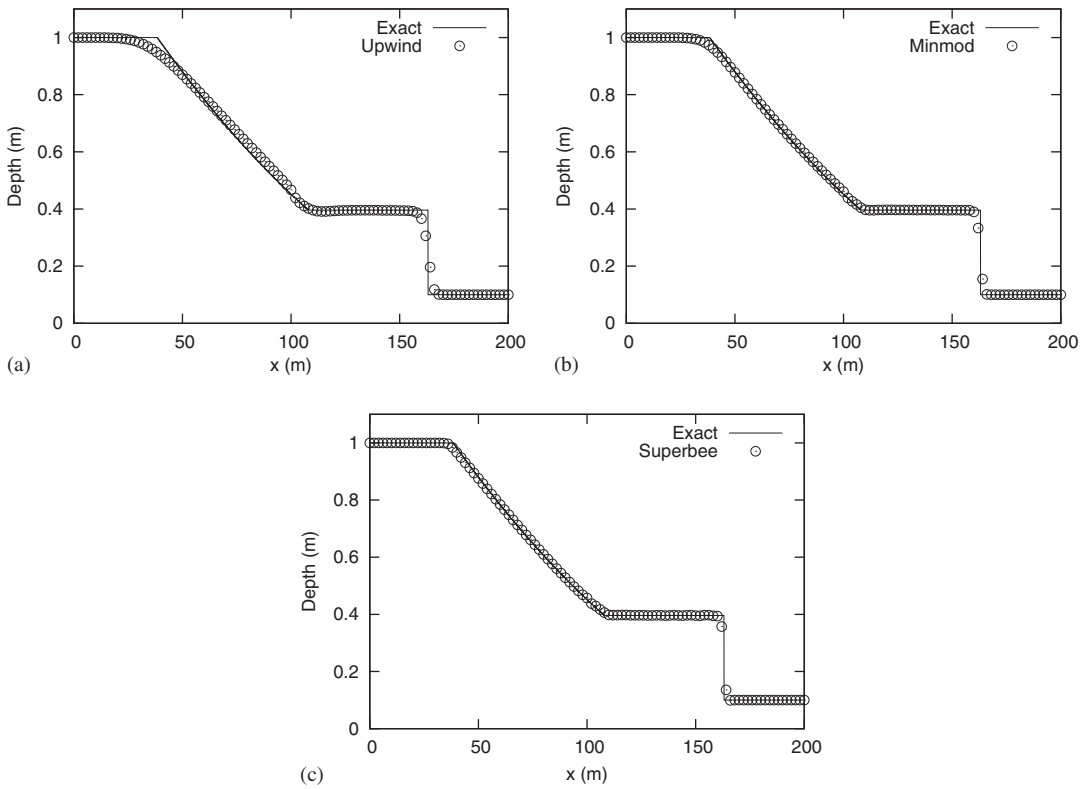

Figure 5. Ideal dambreak depth with the schemes of (a) first-order upwind, (b) and (c) second order in space and time TVD with different flux limiters ((b) 'Minmod' and (c) 'Superbee').

With these definitions for θ the time-step size restrictions due to diffusion are eliminated and the Courant–Friedrichs–Lewy (CFL) number is defined as

$$\Delta t = \mathrm{CFL} \min_i \left[\frac{\delta x}{\beta |u| + \sqrt{c^2 + (\beta^2 - \beta) u^2}} \right]_i^n \tag{79}$$

Figure 4 is a plot of the advection–diffusion results. It can be seen that, for the first-order upwind scheme, the antidiffusivity of the implicit discretization of the diffusion counterbalances the numerical diffusion inherent to the first-order advection scheme leading to an acceptable result. However, the antidiffusivity adds up with the antidiffusivity inherent to the second order in space TVD scheme, producing results of worse quality than the first-order approach, especially with the 'Superbee' limiter. If, at the same time, the increased complexity and reduced size of the time steps required by this scheme are considered, it can be discarded for transport problems. On the other hand, the second order in space and time TVD scheme provides the most accurate results, almost independently of the flux limiter used, with a slight diffusive tendency using the 'Minmod' function and a slight antidiffusive tendency when using the 'Superbee' limiter.

DOI: 10.1002/fld

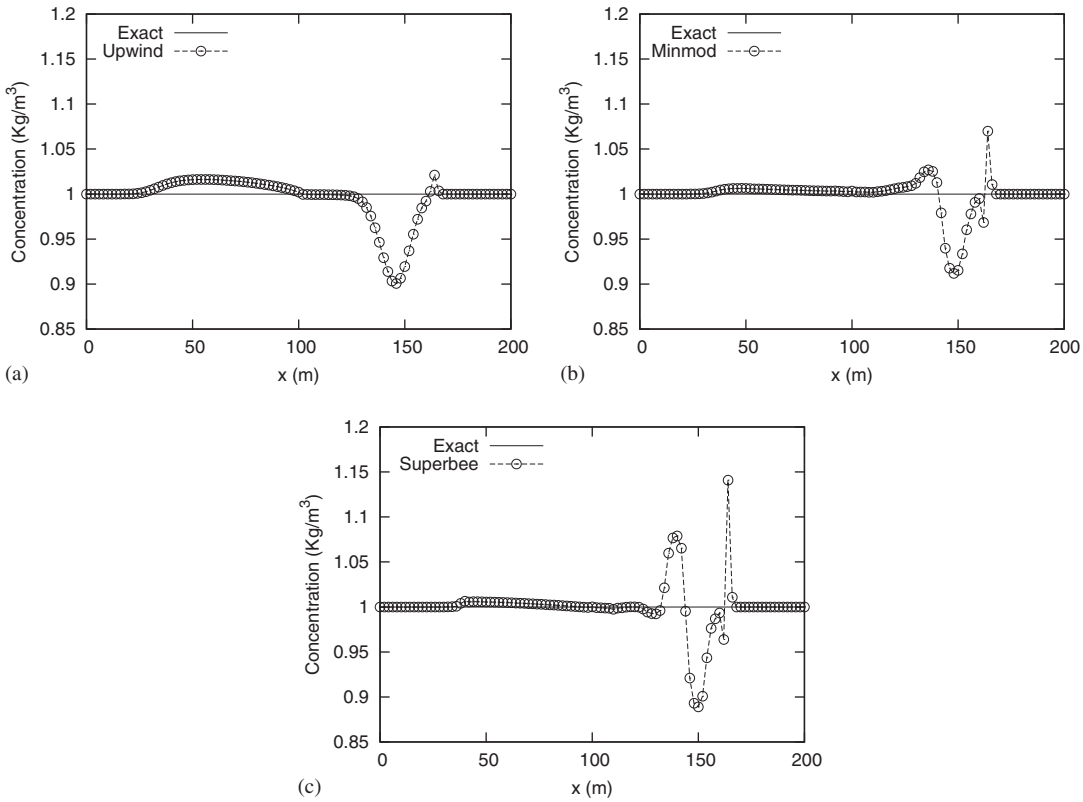

Figure 6. Ideal dambreak concentration with the separated discretization and the schemes of (a) first-order upwind, (b) and (c) second order in space and time TVD with different flux limiters ((b) 'Minmod' and (c) 'Superbee').

7.2. Ideal dambreak with uniform solute concentration and with solute discontinuity

The ideal dambreak problem is one of the classical examples used as test cases for unsteady shallow-water flow simulations. The reason is that for flat and frictionless bottom, rectangular cross-section and no diffusion, the problem defined by zero initial velocity and initial discontinuities in the water depth and solute concentration has an exact solution [24].

A rectangular channel 200 m long and 1 m wide has been considered with an initial depth ratio 1:0.1 m. A grid spacing of $\delta x = 2$ m and CFL $= 0.9$ was used for all the simulations. The plots in Figure 5 show the numerical solution for the water depth from three schemes *versus* the exact solution for $t = 20$ s.

A second case corresponds to the same dambreak discontinuity together with a uniform initial solute concentration of $1\,\mathrm{kg/m^3}$. Figure 6 displays the concentration results for $t = 20$ s using the separated discretization. None of the numerical schemes is able to keep the concentration uniform as time progresses. Figure 7 shows the results obtained with the coupled discretization for the same test case. The first-order upwind scheme preserves the uniform concentration as well as the second-order TVD scheme with different flux limiters, if the characteristic limiting formulation is

DOI: 10.1002/fld

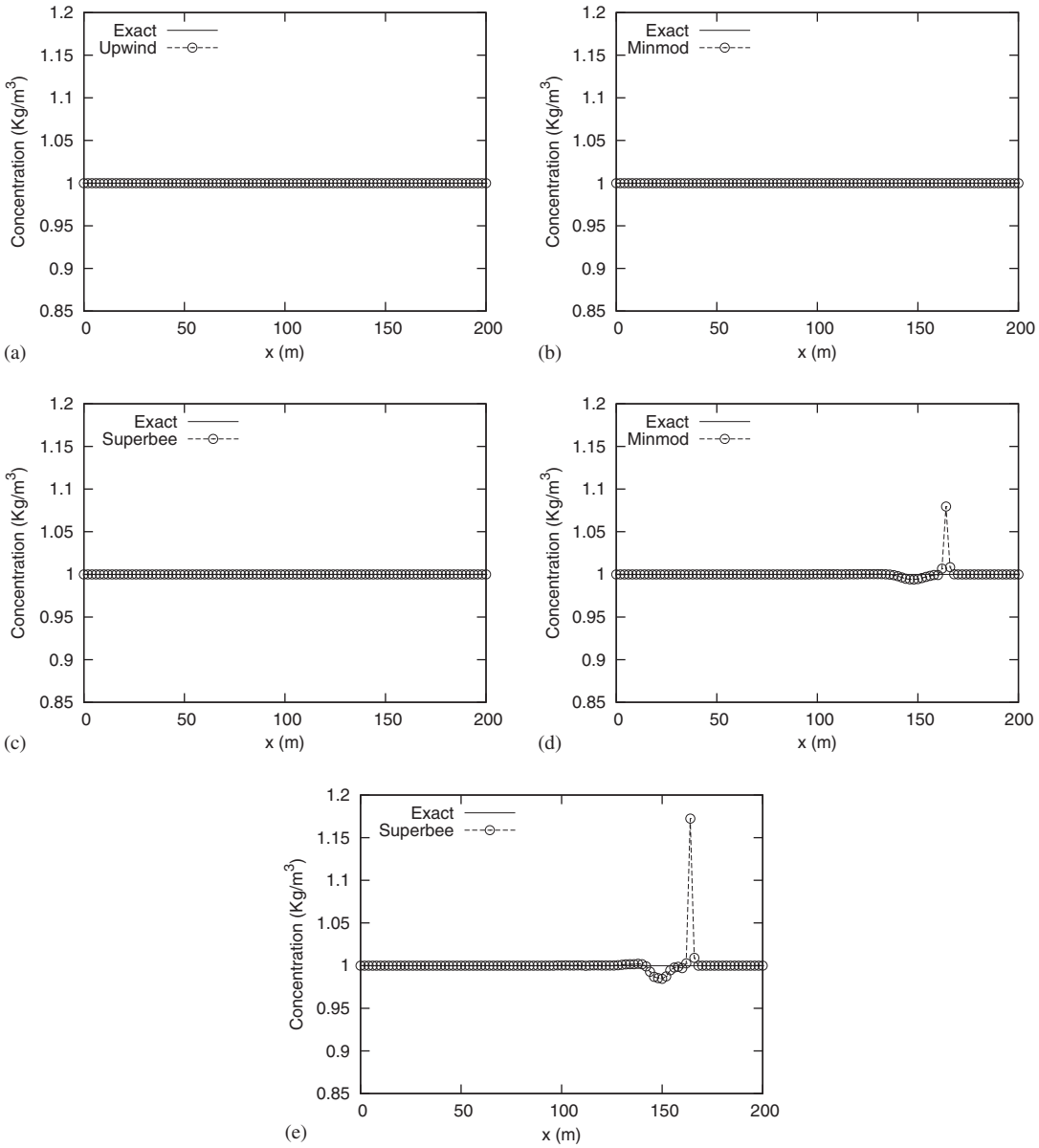

Figure 7. Ideal dambreak concentration with the coupled discretization and the schemes of (a) first-order upwind: (b)–(e) second order in space and time TVD with (b) and (c) characteristic, (d) and (e) vectorial limiting discretization; (b) and (d) 'Minmod', (c) and (e) 'Superbee' flux limiter.

used. When the vectorial limiting discretization is used for the limiters, the numerical solution is not free from oscillations.

As a third dambreak test case, an initial discontinuity in the concentration of $1:0\,\mathrm{kg/m^3}$ in the same location as the depth jump has been considered. Figure 8 shows the results obtained

DOI: 10.1002/fld

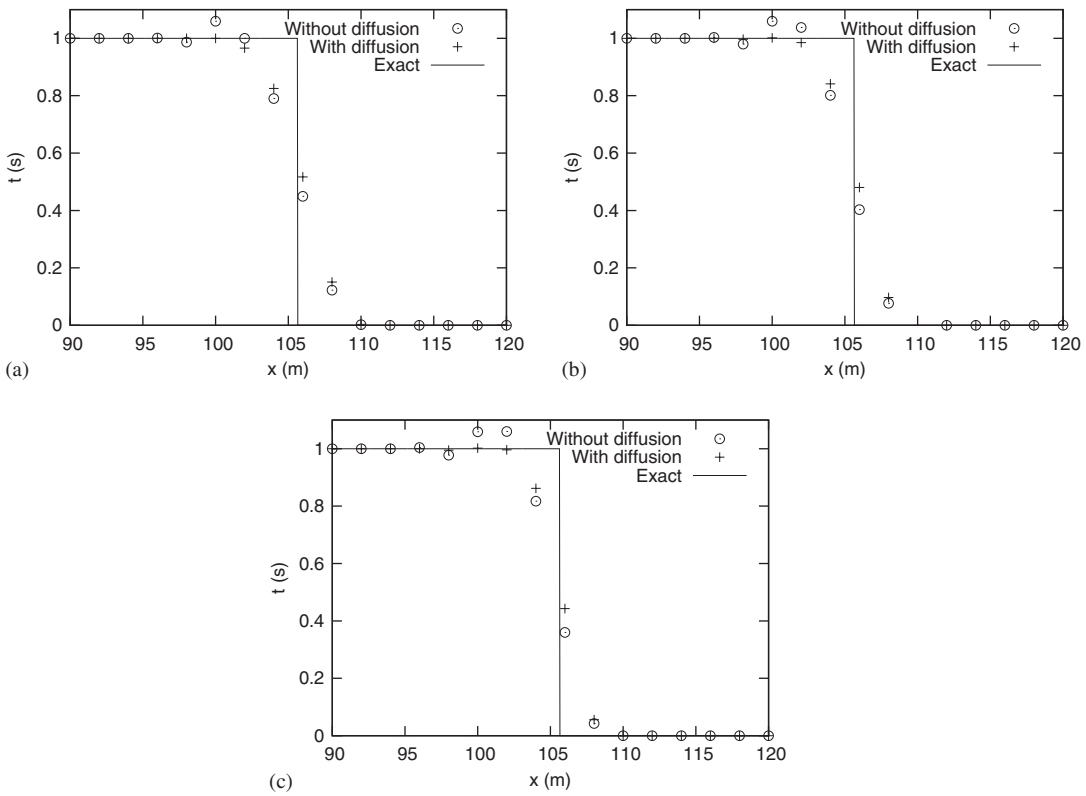

Figure 8. Ideal dambreak discontinuous concentration for $t = 2$ s with the coupled discretization with and without artificial diffusion and the characteristic limiting discretization for: (a) the first-order upwind and the second order in space and time schemes with the flux limiter; (b) 'Minmod'; and (c) 'Superbee'.

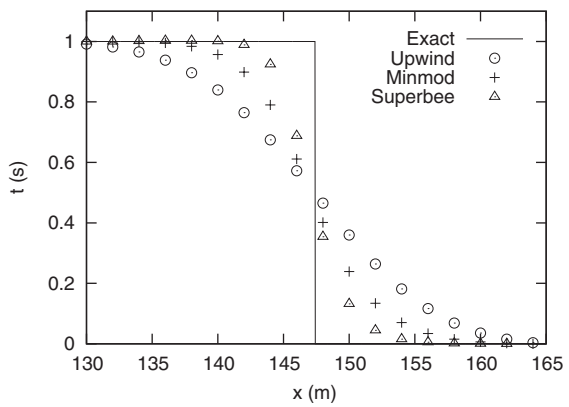

Figure 9. Ideal dambreak discontinuous concentration for $t = 20$ s with the coupled discretization and the characteristic limiting discretization for the first-order upwind and the second order in space and time schemes.

DOI: 10.1002/fld

at $t = 2$ s using the coupled discretization with and without the artificial diffusion described in Section 7. It is clear that without the artificial diffusion slight numerical oscillations appear near the front and that they disappear when using artificial diffusion. Figure 9 shows the results provided by the schemes using the coupled discretization, artificial diffusion and characteristic limiting discretization for $t = 20$ s. The first-order scheme produces more numerical damping than the second-order schemes as expected. Among the limiting functions, 'Superbee' appears slightly more accurate than 'Minmod'.

8. PRACTICAL APPLICATIONS

8.1. Flow and solute transport on an impervious irrigation border

The experimental data from [12] were used to validate the proposed models in cases of steady and unsteady flows in conditions of high relative roughness. In that experiment, a free-draining irrigation border 200 m long and 2 m wide, with a slope of $S_0 = 0.000671$ was constructed and

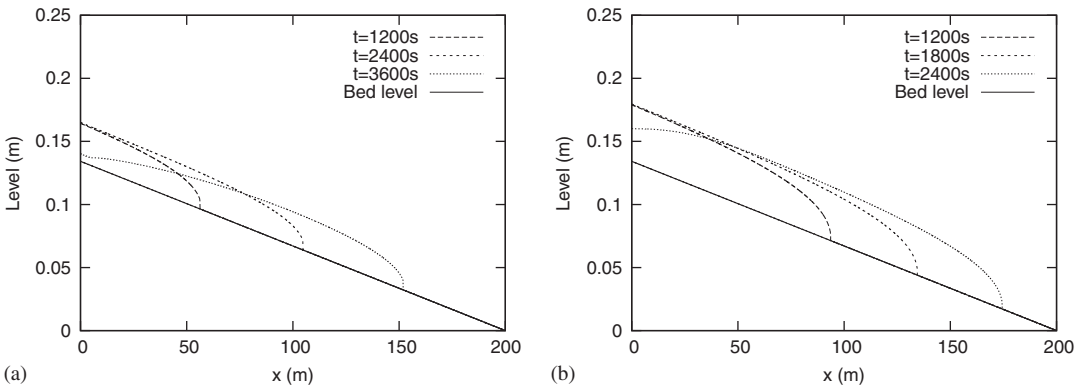

Figure 10. Simulated surface level longitudinal profiles for different times of cases (a) 1 and (b) 2.

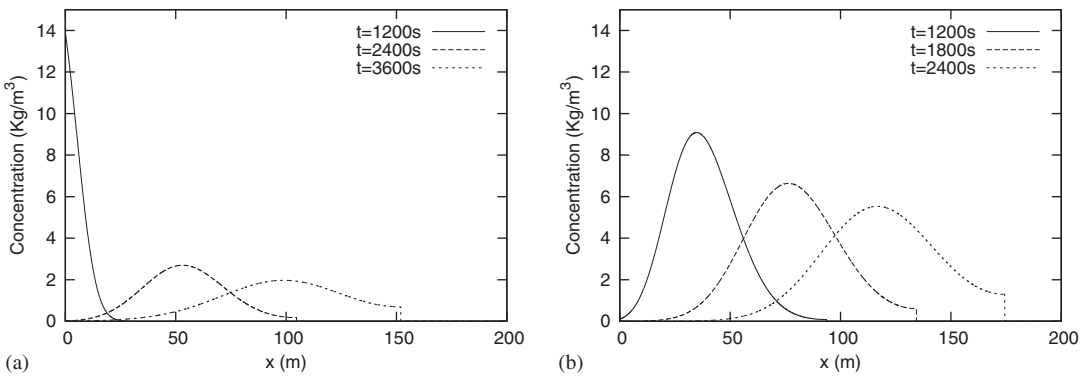

Figure 11. Simulated concentration longitudinal profiles for different times of cases (a) 1 and (b) 2.

DOI: 10.1002/fld

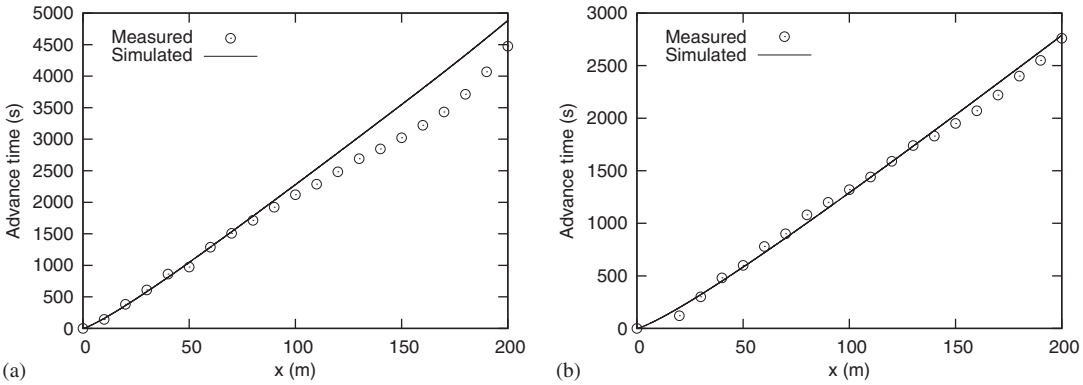

Figure 12. Measured and simulated advance times of cases (a) 1 and (b) 2.

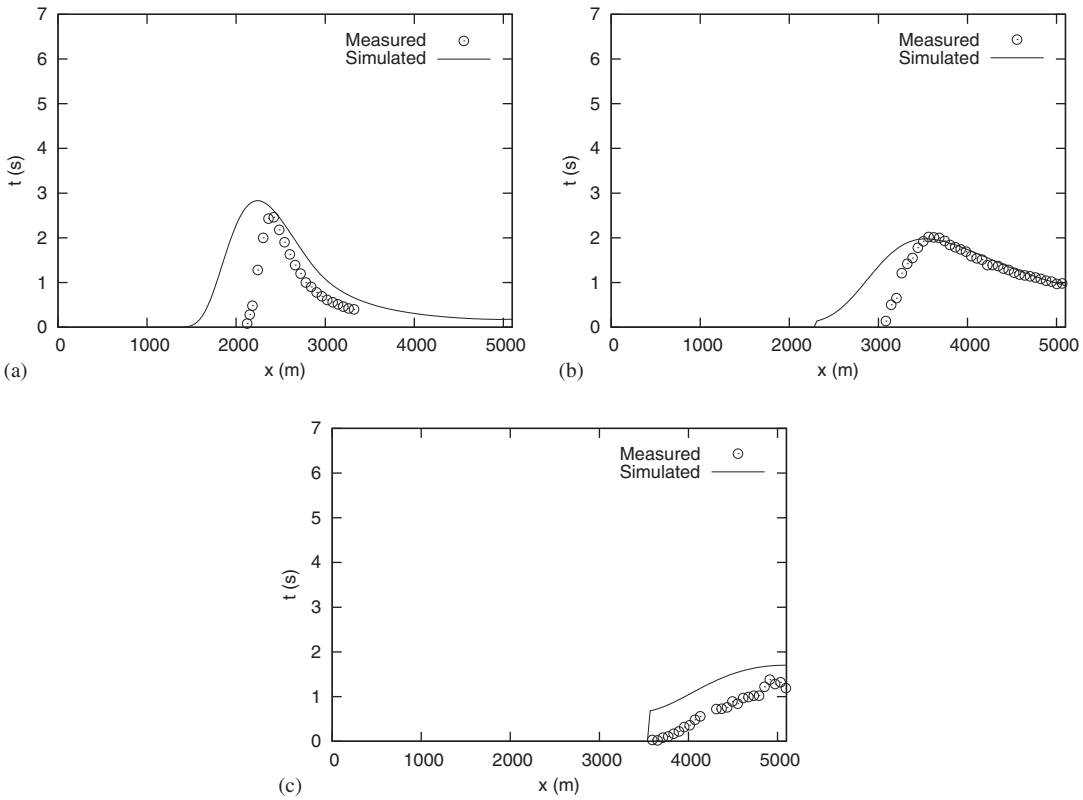

Figure 13. Measured and simulated time evolution of concentration of case 1 at: (a) $x = 50\,\mathrm{m}$; (b) $x = 100\,\mathrm{m}$; and (c) $x = 150\,\mathrm{m}$.

DOI: 10.1002/fld

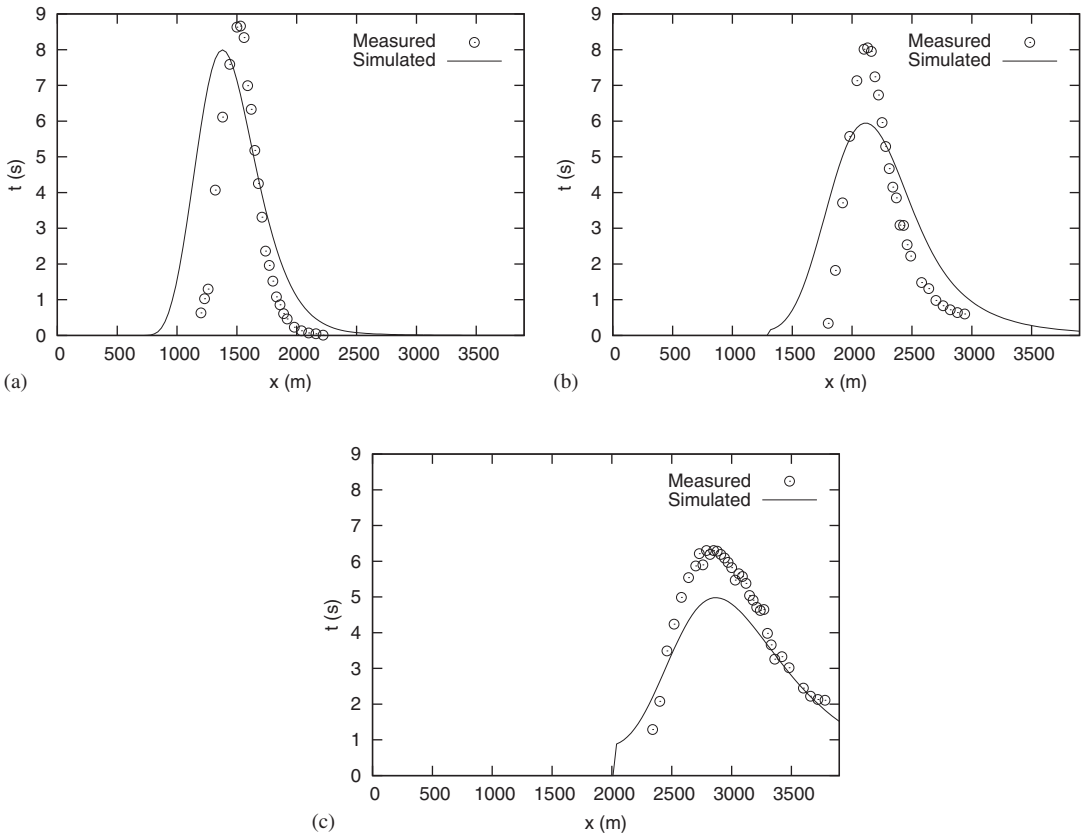

Figure 14. Measured and simulated time evolution of concentration of case 2 at: (a) $x = 50\,\mathrm{m}$; (b) $x = 100\,\mathrm{m}$; and (c) $x = 150\,\mathrm{m}$.

covered with a plastic film. A fine layer gravel (with d_{50} of approximately 20 mm) was added on the top of the plastic film. Two unsteady flow experiments of water flow advancing over the dry border bed were performed and will be simulated for calibration. In case 1, an inlet discharge of $Q = 0.0048\,\mathrm{m}^3/\mathrm{s}$ was applied and, after 1033 s of water application, 7 kg of salt were released during 180 s at the upstream end. The water inlet was interrupted at $t = 2698\,\mathrm{s}$. In case 2, the inlet discharge was $Q = 0.0118\,\mathrm{m}^3/\mathrm{s}$, 28 kg of salt were released during 360 s and the water inflow was interrupted at $t = 2265\,\mathrm{s}$. For the bed roughness simulation, a Manning coefficient $n = 0.09\,\mathrm{s/m}^{1/3}$ was used and, for the longitudinal dispersion coefficient, model (6) was adopted. From the computational point of view, a grid with 2000 nodes was involved, a CFL = 0.9 was fixed all the time and the second order in space and time TVD scheme with characteristic limiting discretization, 'Superbee' flux limiter and artificial diffusion (69) was applied.

In case 1, 5100 s of experiment were simulated and 3900 s in case 2. Figures 10 and 11 show longitudinal profiles of surface level (front advance) and solute concentration, respectively, at different times for both cases. They are useful to see that the selected numerical method is completely free from numerical oscillations even at the locations close to the advancing front.

DOI: 10.1002/fld

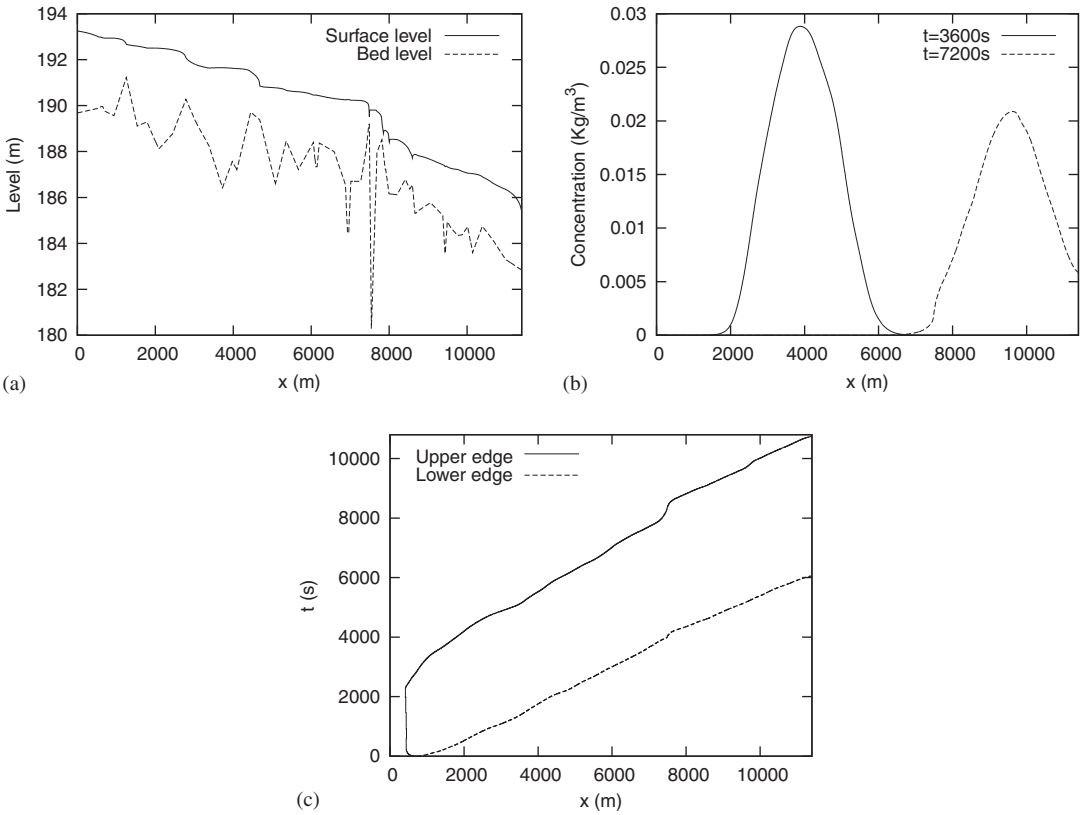

Figure 15. Petrol spill in the Ebro river: (a) longitudinal bed and water surface profiles; (b) longitudinal concentration profiles at 1 and 2 h after the spill; and (c) time evolution of the plume of concentration exceeding the dangerous threshold.

Figure 12 illustrates the good behaviour of the solution in the simulation of the front advance. In both cases, the numerical advance has been compared with the measured advance. Figures 13 and 14 compare the time evolution of the measured and calculated concentration at several gauging points for both cases 1 and 2, respectively. The results indicate that the accuracy provided by this scheme is sufficient for this type of application. The observed differences can be attributed mostly to the diffusion model, although it is remarkable that the simple Rutherford model, proposed for river mixing with very different flow conditions, provides a reasonable approximation without any fitting procedure. The simulation results are satisfactory since they accurately predict the advancing velocity. However, the model overestimates the dispersion effect mainly in case 2.

8.2. Pollutant spill in a river

In order to show the practical application of the model in a river flow context, a hazardous and instantaneous pollutant spill of 20 T of petrol at a point of a 11.4 km reach of the Ebro River will be simulated. The solubility of the petrol at the typical temperature of the river water was estimated as $0.03\,\mathrm{kg/m^3}$. For higher concentrations, the petrol was assumed to precipitate to the

DOI: 10.1002/fld

bottom remaining there. The steady annual base river discharge of $200\,m^3/s$ was assumed. In a first run, the steady-state water surface profile corresponding to that discharge in the river reach was calculated. Figure 15(a) represents the bed and surface levels at steady state. The spill was located at 700 m of the upstream end. Figure 15(b) shows two concentration longitudinal profiles at 1 and 2 h of the spill. The Spanish law establishes that $9.5\,mg/m^3$ is the limit of tolerance for the pernicious influence of petrol concentration in riverine ecological systems. Figure 15(c) represents the time evolution of borders of the contaminant cloud with a concentration exceeding the dangerous limit.

9. CONCLUSIONS

A conservative formulation of the system of equations governing the water flow and the solute transport has been adopted as the basis of our study. The formulation of several finite volume conservative upwind schemes well suited for the numerical simulation of one-dimensional shallow-water flow and solute transport has been provided. Two possibilities have been identified, separate or coupled discretization, leading to different degrees of influence of the flow processes to the solute transport at the discrete level.

It has been proved that well-balanced conservative upwind schemes based on a separate discretization of the scalar solute transport from the shallow-water equations are not able to preserve uniform solute profiles in situations of unsteady subcritical flow even when using first-order methods. However, the coupled formulation and discretization of the system is proved to lead to the correct solution in first-order approximations.

When seeking more accuracy, second-order TVD schemes can be applied. It has been shown that a careful definition of the flux limiter function is required in order to preserve uniform solute profiles in the solute distribution function in cases of unsteady subcritical flow.

The work shows that, in cases of subcritical unsteady irregular flow, the coupled discretization is necessary but nevertheless not sufficient always to ensure concentration distributions free from oscillations and a method of using an artificial diffusion in subcritical cases is proposed.

The validation test cases show the good performance of the second-order TVD schemes for the coupled system formulation in cases of steady and unsteady flows.

APPENDIX A: PROPERTIES OF THE EULERIAN NUMERICAL SCHEMES

A.1. Conservation

The conservative form (1) can be integrated in a time interval T and in a domain length L to obtain a global rule of conservation

$$\int_0^T \int_0^L \left(\frac{\partial \mathbf{U}}{\partial t} + \frac{\partial \mathbf{F}^c}{\partial x} + \frac{\partial \mathbf{D}}{\partial x} \right) \mathrm{d}x\,\mathrm{d}t = \int_0^T \int_0^L \mathbf{S}\,\mathrm{d}x\,\mathrm{d}t$$

$$\Rightarrow \int_0^L \mathbf{U}(x,t)\,\mathrm{d}x - \int_0^L \mathbf{U}(x,0)\,\mathrm{d}x = \int_0^T [\mathbf{F}(0,t) + \mathbf{D}(0,t)]\,\mathrm{d}t - \int_0^T [\mathbf{F}(L,t) + \mathbf{D}(L,t)]\,\mathrm{d}t + \int_0^T \int_0^L \mathbf{S}\,\mathrm{d}x\,\mathrm{d}t \tag{A1}$$

DOI: 10.1002/fld

showing us that the time variation of the conserved variables is equal to the flux entering minus the flux leaving the system plus the contribution of the source terms. When discretizing a conservation law like (1), bad numerical approximations can lead to unacceptable error. Schemes approximating the conservation equation (A1) correctly are called conservative schemes [5]. A definition of a conservative scheme follows the structure proposed by Lax [25]:

$$\Delta \mathbf{U}_i^n = \Delta t \left[\mathbf{S}_i^* - \frac{1}{\delta x} (\mathbf{F}_{i+(1/2)}^* - \mathbf{F}_{i-(1/2)}^*) \right] \tag{A2}$$

where $\mathbf{F}^*$ and $\mathbf{S}^*$ are the numerical flux and source term, respectively, and represent a suitable approximation to the physical flux and source term. Δ will be used for time increments $\Delta f^n = f^{n+1} - f^n$, and δ represents spatial increment $\delta f_{i+(1/2)} = f_{i+1} - f_i$. The schemes so defined are conservative since they produce a good approximation of (A1), provided that the discretization of fluxes and source terms is consistent, that is,

$$\mathbf{F}^* \approx \mathbf{F}^{\mathrm{c}} + \mathbf{D}, \quad \mathbf{S}^* \approx \mathbf{S}^{\mathrm{c}} \tag{A3}$$

Adding up all the increments defined by the numerical scheme (A2) in a grid of N spatial nodes and M time steps, an approximation of the global conservation (A1) is obtained:

$$\begin{aligned}
\sum_{j=0}^{M-1} \sum_{i=1}^{N-1} \Delta \mathbf{U}_i^j \, \delta x &\approx \int_{x_{1/2}}^{x^{N-(1/2)}} \mathbf{U}(x, t^M) \, \mathrm{d}x - \int_{x_{1/2}}^{x^{N-(1/2)}} \mathbf{U}(x, t^0) \, \mathrm{d}x \\
\sum_{j=0}^{M-1} \sum_{i=1}^{N-1} (\mathbf{S}^*)_i^j \, \delta x \Delta t &\approx \int_{t^0}^{t^M} \mathrm{d}t \int_{x_{1/2}}^{x^{N-(1/2)}} \mathbf{S}(x, t) \, \mathrm{d}x \\
-\sum_{j=0}^{M-1} \sum_{i=1}^{N-1} \Delta t [(\mathbf{F}^*)_{i+(1/2)}^j - (\mathbf{F}^*)_{i-(1/2)}^j] &= \sum_{j=0}^{M-1} \Delta t [(\mathbf{F}^*)_{N-(1/2)}^j - (\mathbf{F}^*)_{1/2}^j] \\
&\approx \int_{t^0}^{t^M} [\mathbf{F}^{\mathrm{c}}(x_{1/2}, t) + \mathbf{D}(x_{1/2}, t)] \, \mathrm{d}t \\
&\quad - \int_{t^0}^{t^M} [\mathbf{F}^{\mathrm{c}}(x_{N-(1/2)}, t) + \mathbf{D}(x_{N-(1/2)}, t)] \, \mathrm{d}t
\end{aligned} \tag{A4}$$

A numerical flux $\mathbf{F}^{\mathrm{T}}$ can also be defined at the grid nodes. The difference in this flux across a grid cell can be decomposed into incoming and outgoing parts. The schemes so built follow

$$\begin{aligned}
\delta \mathbf{F}_{i+(1/2)}^{\mathrm{T}} &= \mathbf{F}_{i+1}^{\mathrm{T}} - \mathbf{F}_i^{\mathrm{T}} = \delta \mathbf{F}_{i+(1/2)}^{\mathrm{R}} + \delta \mathbf{F}_{i+(1/2)}^{\mathrm{L}} \\
\Delta \mathbf{U}_i^n &= \Delta t \left[\left(\mathbf{S} - \frac{\delta \mathbf{F}}{\delta x} \right)_{i-(1/2)}^{\mathrm{L}} + \left(\mathbf{S} - \frac{\delta \mathbf{F}}{\delta x} \right)_{i+(1/2)}^{\mathrm{R}} \right]
\end{aligned} \tag{A5}$$

This also leads to conservative schemes since this form can be shown to be equivalent to (A2) and the following interface numerical flux can be defined [5, 6]:

$$\mathbf{F}_{i+(1/2)}^* = \mathbf{F}_i^{\mathrm{T}} + \delta \mathbf{F}_{i+(1/2)}^{\mathrm{R}} = \mathbf{F}_{i+1}^{\mathrm{T}} - \delta \mathbf{F}_{i+(1/2)}^{\mathrm{L}}, \quad \mathbf{S}_i^* = \mathbf{S}_{i+(1/2)}^{\mathrm{L}} + \mathbf{S}_{i-(1/2)}^{\mathrm{R}} \tag{A6}$$

DOI: 10.1002/fld

A conservative scheme can be derived by discretizing the characteristic form of Equation (14):

$$\Delta \mathbf{W}_i^n = \Delta t \left\{ \mathbf{\Phi}_{i-(1/2)}^{\mathrm{L}} \left(\mathbf{P}^{-1}\mathbf{S}^{\mathrm{nc}} - \mathbf{\Lambda}\frac{\delta \mathbf{W}}{\delta x} \right)_{i-(1/2)} + \mathbf{\Phi}_{i+(1/2)}^{\mathrm{R}} \left(\mathbf{P}^{-1}\mathbf{S}^{\mathrm{nc}} - \mathbf{\Lambda}\frac{\delta \mathbf{W}}{\delta x} \right)_{i+(1/2)} - \frac{\mathbf{P}^{-1}}{\delta x}(\mathbf{D}_{i+(1/2)}^{\mathrm{R}} - \mathbf{D}_{i-(1/2)}^{\mathrm{L}}) \right\} \tag{A7}$$

with $\mathbf{\Phi}_{i+(1/2)}^{\mathrm{L,R}}$ being the characteristic decomposition matrices. Multiplying back by $\mathbf{P}$ in order to recover the physical variables, extracting $\mathbf{P}^{-1}$ and using (11), (A7) can be written as

$$\Delta \mathbf{U}_i^n = \Delta t \left\{ \left[\mathbf{P}\mathbf{\Phi}^{\mathrm{R}}\mathbf{P}^{-1} \left(\mathbf{S}^{\mathrm{nc}} - \mathbf{J}\frac{\delta \mathbf{U}}{\delta x} \right) \right]_{i+(1/2)} + \left[\mathbf{P}\mathbf{\Phi}^{\mathrm{L}}\mathbf{P}^{-1} \left(\mathbf{S}^{\mathrm{nc}} - \mathbf{J}\frac{\delta \mathbf{U}}{\delta x} \right) \right]_{i+(1/2)} - \frac{1}{\delta x}(\mathbf{D}_{i+(1/2)}^{\mathrm{R}} - \mathbf{D}_{i-(1/2)}^{\mathrm{L}}) \right\} \tag{A8}$$

This scheme will be conservative if the following condition at the discrete level is enforced [6]:

$$\mathbf{G}_{i+(1/2)}^n = \left(\mathbf{S}^{\mathrm{nc}} - \mathbf{J}\frac{\partial \mathbf{U}}{\partial x} \right)_{i+(1/2)} = \left(\mathbf{S}^{\mathrm{qc}} - \frac{\partial \mathbf{F}^{\mathrm{qc}}}{\partial x} \right)_{i+(1/2)} = \left(\mathbf{S}^{\mathrm{c}} - \frac{\partial \mathbf{F}^{\mathrm{c}}}{\partial x} \right)_{i+(1/2)} \tag{A9}$$

which holds provided that

$$\begin{aligned} (I_2)_{i+(1/2)} &= \delta(I_1)_{i+(1/2)} - A_{i+(1/2)}\delta h_{i+(1/2)} \\ u_{i+(1/2)} &= \frac{\sqrt{A_{i+1}}u_{i+1} + \sqrt{A_i}u_i}{\sqrt{A_{i+1}} + \sqrt{A_i}}, \quad s_{i+(1/2)} = \frac{\sqrt{A_{i+1}}s_{i+1} + \sqrt{A_i}s_i}{\sqrt{A_{i+1}} + \sqrt{A_i}} \end{aligned} \tag{A10}$$

In order to complete the formulation, the choice of some average values remains open. The simplest option has been used in this work:

$$A_{i+(1/2)} = \frac{A_{i+1} + A_i}{2}, \quad \beta_{i+(1/2)} = \frac{\beta_{i+1} + \beta_i}{2}, \quad c_{i+(1/2)} = \sqrt{g\frac{A_{i+1} + A_i}{B_{i+1} + B_i}} \tag{A11}$$

The conservative decomposition matrices will be defined as

$$\mathbf{\Omega}^{\mathrm{R,L}} = \mathbf{P}\mathbf{\Phi}^{\mathrm{R,L}}\mathbf{P}^{-1}, \quad \mathbf{\Omega}^{\mathrm{R}} + \mathbf{\Omega}^{\mathrm{L}} = \mathbf{\Phi}^{\mathrm{R}} + \mathbf{\Phi}^{\mathrm{L}} = \mathbf{1} \tag{A12}$$

By defining, at the same time, the vectors

$$\mathbf{G}^{\mathrm{R,L}} = \mathbf{\Omega}^{\mathrm{R,L}}\mathbf{G} \tag{A13}$$

the non-conservative, quasi-conservative and conservative forms of this scheme can be written as follows:

$$\Delta \mathbf{U}_i^n = \Delta t \left[\mathbf{G}_{i+(1/2)}^{\mathrm{R}} + \mathbf{G}_{i-(1/2)}^{\mathrm{L}} - \frac{1}{\delta x}(\mathbf{D}_{i+(1/2)}^{\mathrm{R}} - \mathbf{D}_{i-(1/2)}^{\mathrm{L}}) \right] \tag{A14}$$

Since the three forms are equivalent, the simplest quasi-conservative is recommended [6].

DOI: 10.1002/fld

The considered numerical schemes are conservative since they admit the following wave decomposition:

- First-order upwind scheme with implicit diffusion:

$$\mathbf{F}_i^{\mathrm{T}} = (\mathbf{F}^{\mathrm{c}})_i^n, \quad \mathbf{G}_{i+(1/2)}^{\mathrm{L}} = \left(\mathbf{G}^+ - \nu\frac{\delta\mathbf{U}}{\delta x}\right)_{i+(1/2)}^n + \frac{1}{\delta x}\mathbf{D}_{i+(1/2)}^{n+\theta}$$
$$\mathbf{G}_{i+(1/2)}^{\mathrm{R}} = \left(\mathbf{G}^- + \nu\frac{\delta\mathbf{U}}{\delta x}\right)_{i+(1/2)}^n - \frac{1}{\delta x}\mathbf{D}_{i+(1/2)}^{n+\theta} \tag{A15}$$

- Second order in space and time TVD scheme with implicit diffusion and vectorial limiting discretization:

$$\begin{aligned}\mathbf{F}_i^{\mathrm{T}} &= (\mathbf{F}^{\mathrm{c}})_i^n \\ \mathbf{G}_{i+(1/2)}^{\mathrm{L}} &= \left(\mathbf{G}^+ - \nu\frac{\delta\mathbf{U}}{\delta x}\right)_{i+(1/2)}^n - \frac{1}{2}(\boldsymbol{\Psi}^+\mathbf{E}^+)_{i-(1/2)}^n + \frac{1}{2}(\boldsymbol{\Psi}^-\mathbf{E}^-)_{i+(3/2)}^n \\ &\quad + \frac{1}{\delta x}\mathbf{D}_{i+(1/2)}^{n+\theta} \\ \mathbf{G}_{i+(1/2)}^{\mathrm{R}} &= \left(\mathbf{G}^- + \nu\frac{\delta\mathbf{U}}{\delta x}\right)_{i+(1/2)}^n + \frac{1}{2}(\boldsymbol{\Psi}^+\mathbf{E}^+)_{i-(1/2)}^n - \frac{1}{2}(\boldsymbol{\Psi}^-\mathbf{E}^-)_{i+(3/2)}^n \\ &\quad - \frac{1}{\delta x}\mathbf{D}_{i+(1/2)}^{n+\theta}\end{aligned} \tag{A16}$$

- Second order in space and time TVD scheme with implicit diffusion and characteristic limiting discretization:

$$\begin{aligned}\mathbf{F}_i^{\mathrm{T}} &= (\mathbf{F}^{\mathrm{c}})_i^n \\ \mathbf{G}_{i+(1/2)}^{\mathrm{L}} &= \left(\mathbf{G}^+ - \nu\frac{\delta\mathbf{U}}{\delta x}\right)_{i+(1/2)}^n - \frac{1}{2}(\mathbf{P}\boldsymbol{\Psi}^+\mathbf{L}^+)_{i-(1/2)}^n + \frac{1}{2}(\mathbf{P}\boldsymbol{\Psi}^-\mathbf{L}^-)_{i+(3/2)}^n \\ &\quad + \frac{1}{\delta x}\mathbf{D}_{i+(1/2)}^{n+\theta} \\ \mathbf{G}_{i+(1/2)}^{\mathrm{R}} &= \left(\mathbf{G}^- + \nu\frac{\delta\mathbf{U}}{\delta x}\right)_{i+(1/2)}^n + \frac{1}{2}(\mathbf{P}\boldsymbol{\Psi}^+\mathbf{L}^+)_{i-(1/2)}^n - \frac{1}{2}(\mathbf{P}\boldsymbol{\Psi}^-\mathbf{L}^-)_{i+(3/2)}^n \\ &\quad - \frac{1}{\delta x}\mathbf{D}_{i+(1/2)}^{n+\theta}\end{aligned} \tag{A17}$$

A.2. TVD property

A general three-point scheme, applied to a scalar advection–diffusion equation, can be expressed as

$$\Delta U_i^n + A^-\delta U_{i+(1/2)}^{n+1} + A^+\delta U_{i-(1/2)}^{n+1} = B^-\delta U_{i+(1/2)}^n + B^+\delta U_{i-(1/2)}^n \tag{A18}$$

Even though linear stability and numerical dissipation prevent any amplification of the perturbations, they do not remove oscillations completely from the numerical solution. The total variation

DOI: 10.1002/fld

diminishing property was defined to meet this goal. Starting from the definition of the 'Total Variation' of a numerical solution as

$$\mathrm{TV}^n = \sum_i |\delta U^n_{i+(1/2)}| \tag{A19}$$

a numerical scheme is said to be TVD ('Total Variation Diminishing') if [18]

$$\mathrm{TV}^{n+1} \leqslant \mathrm{TV}^n \tag{A20}$$

Sufficient conditions (although not necessary) for ensuring that a general scheme like (A18) applied to the linear scalar equation is TVD are [18]

$$A^- \leqslant 0, \quad A^+ \geqslant 0, \quad B^- \geqslant 0, \quad B^+ \leqslant 0, \quad B^- - B^+ \leqslant 1 \tag{A21}$$

An unstable scheme cannot be TVD.

Making a linearized analysis, with A, K and u constants, the following coefficients of the general scheme (A18) can be defined for the considered schemes:

- First-order upwind scheme with implicit diffusion:

$$\begin{aligned} &A^+ = \theta\frac{K\Delta t}{\delta x^2}, \quad A^- = -\theta\frac{K\Delta t}{\delta x^2}, \quad B^+ = -\frac{u^+\Delta t}{\delta x} - (1-\theta)\frac{K\Delta t}{\delta x^2} \\ &B^- = -\frac{u^-\Delta t}{\delta x} + (1-\theta)\frac{K\Delta t}{\delta x^2} \end{aligned} \tag{A22}$$

- Second order in space TVD scheme with implicit diffusion:

$$\begin{aligned} &A^+ = \theta\frac{K\Delta t}{\delta x^2}, \quad A^- = -\theta\frac{K\Delta t}{\delta x^2} \\ &B^+_{i+(1/2)} = -\left[1 + \frac{1}{2}(\Psi^+)^n_{i+(1/2)} - \frac{1}{2}\frac{(\Psi^+\delta T^+)^n_{i-(1/2)}}{(\delta T^+)^n_{i+(1/2)}}\right]\frac{u^+\Delta t}{\delta x} - (1-\theta)\frac{K\Delta t}{\delta x^2} \\ &B^-_{i+(1/2)} = -\left[1 + \frac{1}{2}(\Psi^-)^n_{i+(1/2)} - \frac{1}{2}\frac{(\Psi^-\delta T^-)^n_{i+(3/2)}}{(\delta T^-)^n_{i+(1/2)}}\right]\frac{u^-\Delta t}{\delta x} + (1-\theta)\frac{K\Delta t}{\delta x^2} \end{aligned} \tag{A23}$$

- Second order in space and time TVD scheme with implicit diffusion:

$$\begin{aligned} &A^+ = \theta\frac{K\Delta t}{\delta x^2}, \quad A^- = -\theta\frac{K\Delta t}{\delta x^2} \\ &B^+_{i+(1/2)} = -\left\{1 + \frac{1}{2}(1-\sigma)^n_{i+(1/2)}\left[(\Psi^+)^n_{i+(1/2)} - \frac{(\Psi^+\delta E^+)^n_{i-(1/2)}}{(\delta E^+)^n_{i+(1/2)}}\right]\right\}(\sigma^+)^n_{i+(1/2)} \\ &\qquad - (1-\theta)\frac{K\Delta t}{\delta x^2} \\ &B^-_{i+(1/2)} = -\left\{1 + \frac{1}{2}(1+\sigma)^n_{i+(1/2)}\left[(\Psi^-)^n_{i+(1/2)} - \frac{(\Psi^-\delta E^-)^n_{i+(3/2)}}{(\delta E^-)^n_{i+(1/2)}}\right]\right\}(\sigma^-)^n_{i+(1/2)} \\ &\qquad + (1-\theta)\frac{K\Delta t}{\delta x^2} \end{aligned} \tag{A24}$$

DOI: 10.1002/fld

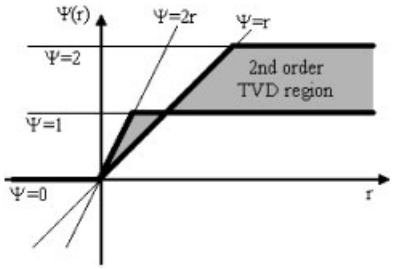

Figure A1. Second-order TVD region for the flux limiter functions.

Applying the TVD conditions (A21) to second order in space TVD scheme with implicit diffusion, the flux limiter will be a positive function so that

$$\Psi(r)=0 \ \ \forall r<0, \quad \Psi(r)\leqslant 2r \ \ \forall r>0 \tag{A25}$$

and this leads to the following conditions:

$$0\leqslant\theta\leqslant 1, \quad \Delta t\leqslant\frac{\delta x^2}{[1+\frac{1}{2}\max(\Psi)]|u|\delta x+(1-\theta)2K} \tag{A26}$$

It is usual to establish the restriction $\Psi(r)\leqslant 2$ in order to be able to work with time-step sizes up to $\Delta t\leqslant\delta x/2|u|$. The intersection between the second-order region and the TVD region for the flux limiter functions in the second order in space TVD scheme is represented in Figure A1. Many particular flux limiter functions are defined in previous works [26–28]. We use the extreme values:

- 'Superbee' [26]: $\Psi(r)=\max[0,\min(1,2r),\min(2,r)]$
- 'Minmod' [26]: $\Psi(r)=\max[0,\min(1,r)]$

Applying the TVD conditions (A21) to second order in space and time TVD scheme with implicit diffusion, the flux limiter will be a positive function so that

$$\Psi(r)=0 \ \ \forall r<0, \quad \Psi(r)\leqslant 2r \ \ \forall r>0, \quad \Psi(r)\leqslant 2 \ \ \forall r \tag{A27}$$

The intersection between the second-order region and the TVD region for the flux limiter functions in the second order in space and time TVD scheme is identical to the second order in space TVD region, shown in Figure A1, and the flux limiter functions defined are also valid for this scheme. Applying conditions (A21) to first-order upwind and second order in space and time TVD schemes with implicit diffusion, both are TVD for

$$0\leqslant\theta\leqslant 1, \quad \Delta t\leqslant\frac{\delta x^2}{|u|\delta x+(1-\theta)2K} \tag{A28}$$

DOI: 10.1002/fld

REFERENCES

1. Thomann RV. Effect of longitudinal dispersion on dynamic water quality response of streams and rivers. *Water Resources Research* 1973; **9**(2):355–366.
2. Rutherford JC. *River Mixing*. Wiley: New York, 1994.
3. Glaister P. Approximate Riemann solutions of the shallow water equations. *Journal of Hydraulic Research* 1988; **26**(3):293–306.
4. Bermúdez A, Vázquez Cendón ME. Upwind methods for hyperbolic conservation laws with source terms. *Computers & Fluids* 1994; **23**(8):1049–1071.
5. Burguete J, García-Navarro P. Efficient construction of high-resolution TVD conservative schemes for equations with source terms: application to shallow water flows. *International Journal for Numerical Methods in Fluids* 2001; **37**(2):209–248.
6. Burguete J, García-Navarro P. Improving simple explicit methods for unsteady open channel and river flow. *International Journal for Numerical Methods in Fluids* 2004; **45**(2):125–156.
7. Rasch PJ, Williamson DL. On shape-preserving interpolation and semi-Lagrangian transport. *SIAM Journal on Scientific and Statistical Computing* 1990; **11**(4):656–687.
8. Karpik SR, Crockett SR. Semi-Lagrangian algorithm for two-dimensional advection–diffusion equations on curvilinear coordinate meshes. *Journal of Hydraulic Engineering* (ASCE) 1997; **123**(5):389–401.
9. Néelz S, Wallis SG. Tracking accuracy of a semi-Lagrangian method for advection–dispersion modelling in rivers. *International Journal for Numerical Methods in Fluids* 2007; **53**(1):1–21.
10. Islam MR, Chaudry MH. Numerical solution of transport equation for applications in environmental hydraulics and hydrology. *Journal of Hydrology* 1997; **191**:106–121.
11. Komatsu T, Ohgushi K, Asai K. Refined numerical scheme for advective transport in diffusion simulation. *Journal of Hydraulic Engineering* (ASCE) 1997; **123**(1):41–50.
12. García-Navarro P, Playán E, Zapata N. Solute transport modelling in overland flow applied to fertigation. *Journal of Irrigation and Drainage Engineering* (ASCE) 2000; **126**(1):33–40.
13. Murillo J, Burguete J, Brufau P, García-Navarro P. Coupling between shallow water and solute flow equations: analysis and management of source terms in 2D. *International Journal for Numerical Methods in Fluids* 2005; **49**(3):267–299.
14. Cao Z, Meng J, Pender G, Wallis S. Flow resistance and momentum flux in compound open channels. *Journal of Hydraulic Engineering* (ASCE) 2006; **132**(12):1272–1282.
15. Burguete J, García-Navarro P, Murillo J, García-Palacín I. Analysis of the friction term in the one-dimensional shallow-water model. *Journal of Hydraulic Engineering* (ASCE) 2007; **133**(9).
16. Gauckler PG. Études théoriques et practiques sur l'écoulement et le mouvement des eaux. *Comptes Rendues de l'Académie des Sciences*, *Paris* 1867; **64**:818–822.
17. Manning R. *On the Flow of Water in Open Channels and Pipes*. Institution of Civil Engineers of Ireland: Ireland, 1890.
18. Hirsch C. *Computational Methods for Inviscid and Viscous Flows*: *Numerical Computation of Internal and External Flows*. Wiley: New York, 1990.
19. Sweby PK. High resolution schemes using flux limiters for hyperbolic conservation laws. *SIAM Journal on Numerical Analysis* 1984; **21**(5):995–1011.
20. Harten A, Hyman JM. Self adjusting grid methods for one-dimensional hyperbolic conservation laws. *Journal of Computational Physics* 1983; **50**(2):235–269.
21. Burguete J, García-Navarro P. Implicit schemes with large time steps for non-linear equations: application to river flow hydraulics. *International Journal for Numerical Methods in Fluids* 2004; **46**(6): 607–636.
22. Burguete J, García-Navarro P, Aliod R. Numerical simulation of runoff from extreme rainfall events in a mountain water cachment. *Natural Hazards in Earth System Sciences* 2002; **2**:1–9.
23. Burguete J, García-Navarro P, Murillo J. Numerical boundary conditions for globally mass conservative methods to solve the shallow-water equations and applied to river flow. *International Journal for Numerical Methods in Fluids* 2006; **51**(6):585–615.
24. Stoker JJ. *Water Waves*. Interscience: New York, 1957.
25. Lax PD. Hyperbolic systems of conservation laws II. *Communication on Pure and Applied Mathematics* 1957; **10**:537–566.

DOI: 10.1002/fld

26. Roe PL. Generalized formulation of TVD Lax–Wendroff schemes. *ICASE Report 84-53*, *NASA CR-172478*, NASA Langley Research Center, 1984.
27. van Albada GD, van Leer B, Roberts WW. A comparative study of computational methods in cosmic gas dynamics. *Astronomy & Astrophysics* 1982; **108**:76–84.
28. van Leer B. Towards the ultimate conservative difference scheme II. Monotonicity, conservation combined in a second order scheme. *Journal of Computational Physics* 1974; **14**:361–370.

DOI: 10.1002/fld